

# NAVAL POSTGRADUATE SCHOOL Monterey, California



## THESIS

CORROSION MECHANISMS AND BEHAVIOR OF  
A P-130X GR/6063 AL  
COMPOSITE IN AQUEOUS ENVIRONMENTS

by

Leslie R. Elkin

September 1990

Thesis Advisor

Indranath Dutta

Approved for public release; distribution is unlimited.



Unclassified

Security classification of this page

## REPORT DOCUMENTATION PAGE

Report Security Classification Unclassified		1b Restrictive Markings	
Security Classification Authority		3 Distribution/Availability of Report	
Declassification Downgrading Schedule		Approved for public release; distribution is unlimited.	
Performing Organization Report Number(s)		5 Monitoring Organization Report Number(s)	
Name of Performing Organization Naval Postgraduate School	6b Office Symbol (if applicable) 34	7a Name of Monitoring Organization Naval Postgraduate School	
Address (city, state, and ZIP code) Monterey, CA 93943-5000		7b Address (city, state, and ZIP code) Monterey, CA 93943-5000	
Name of Funding Sponsoring Organization	8b Office Symbol (if applicable)	9 Procurement Instrument Identification Number	
Address (city, state, and ZIP code)		10 Source of Funding Numbers	
		Program Element No	Project No Task No Work Unit Accession No
Title (include security classification) CORROSION MECHANISMS AND BEHAVIOR OF A P-130X GR/6063 AL COMPOSITE IN AQUEOUS ENVIRONMENTS			
Personal Author(s) Leslie R. Elkin			
Type of Report Master's Thesis	13b Time Covered From To	14 Date of Report (year, month, day) September 1990	15 Page Count 63
Supplementary Notation The views expressed in this thesis are those of the author and do not reflect the official policy or position of the Department of Defense or the U.S. Government.			
Cosati Codes		18 Subject Terms (continue on reverse if necessary and identify by block number)	
Field	Group	Subgroup	
		corrosion, composite, aluminum/graphite composite	
Abstract (continue on reverse if necessary and identify by block number)			
<p>The corrosion mechanisms and behavior of a P-130x graphite fiber reinforced 6063 aluminum composite laminate were studied. Electrochemical and total immersion tests were performed on the composite in 3.5% sodium chloride and 5.0% sodium sulfate solutions. The effects of pH, the presence of sulfite ions, various heat treatments, and electrolyte aeration were investigated. Some tests were also performed on control monolithic 6063 aluminum specimens.</p> <p>Immersion tests showed that when graphite fibers are exposed simultaneously with the matrix, then galvanic coupling is the principal corrosion mechanism in this composite. However, if the composite cross sectional edges are sealed from contact with the environment, then pitting attack of the surface foils becomes the principal mode of attack, especially in harsh environments (chloride and sulfite ions present in addition to low pH). This form of attack can eventually lead to galvanic corrosion. Low pH and the addition of sulfite ion significantly increase the susceptibility to localized corrosion and the rates of both general and galvanic corrosion. Progressive aging of the composite matrix decreases general corrosion rates in deaerated solutions. Electrolyte aeration results in a significant reduction in the composite's resistance to all forms of corrosion.</p>			
Distribution/Availability of Abstract Unclassified unlimited <input type="checkbox"/> same as report <input type="checkbox"/> DTIC users		21 Abstract Security Classification Unclassified	
Name of Responsible Individual Adranath Dutta		22b Telephone (include Area code) (408) 646-2851	22c Office Symbol ME/Du

Approved for public release; distribution is unlimited.

Corrosion Mechanisms and Behavior of a P-130x Gr/6063 Al  
Composite in Aqueous Environments

by

Leslie R. Elkin  
Lieutenant, United States Navy  
B.S., Purdue University, 1984

Submitted in partial fulfillment of the  
requirements for the degree of

MASTER OF SCIENCE IN MECHANICAL ENGINEERING

from the

NAVAL POSTGRADUATE SCHOOL  
September 1990

Anthony J. Healey, Chairman.  
Department of Mechanical Engineering

## ABSTRACT

The corrosion mechanisms and behavior of a P-130x graphite fiber reinforced 6063 aluminum composite laminate were studied. Electrochemical and total immersion tests were performed on the composite in 3.5% sodium chloride and 5.0% sodium sulfate solutions. The effects of pH, the presence of sulfite ions, various heat treatments, and electrolyte aeration were investigated. Some tests were also performed on control monolithic 6063 aluminum specimens.

Immersion tests showed that when graphite fibers are exposed simultaneously with the matrix, then galvanic coupling is the principal corrosion mechanism in this composite. However, if the composite cross sectional edges are sealed from contact with the environment, then pitting attack of the surface foils becomes the principal mode of attack, especially in harsh environments (chloride and sulfite ions present in addition to low pH). This form of attack can eventually lead to galvanic corrosion. Low pH and the addition of sulfite ion significantly increase the susceptibility to localized corrosion and the rates of both general and galvanic corrosion. Progressive aging of the composite matrix decreases general corrosion rates in deaerated solutions. Electrolyte aeration results in a significant reduction in resistance to all forms of corrosion.



## TABLE OF CONTENTS

I. INTRODUCTION.....	1
A. CORROSION OF ALUMINUM ALLOYS--MECHANISMS AND BEHAVIOR..	2
B. CORROSION MECHANISMS AND BEHAVIOR OF MMC'S.....	6
C. RESEARCH OBJECTIVES AND OVERVIEW.....	10
II. EXPERIMENTAL MATERIALS AND PROCEDURE.....	11
A. MATERIALS.....	11
B. SAMPLE PREPARATION AND ELECTRODE FABRICATION.....	13
1. Composite and 6063 Monolithic Aluminum.....	13
2. Graphite Fiber Electrodes.....	14
C. EXPERIMENTAL.....	14
1. Data Acquisition Equipment.....	14
2. Electrochemical Technique Parameters.....	15
a. Corrosion Potential Test Parameters.....	15
b. Galvanic Corrosion Test Parameters.....	15
c. Galvanodynamic Test Parameters.....	16
d. Polarization Resistance Test Parameters.....	16
e. Potentiodynamic Test Parameters.....	17
3. Behavior Study Tests.....	18
4. Immersion Tests.....	19
III. MECHANISM STUDY.....	20
A. RESULTS.....	20
1. Immersion Tests.....	20
a. Edge Protected Samples.....	20

b. Non Edge Protected Samples.....	26
2. Electrochemical Test Results.....	30
a. Polarization Test Plots.....	30
b. Polarization Test Micrographs.....	34
B. MECHANISM DISCUSSION.....	37
IV. EFFECT OF ENVIRONMENTAL AND MATERIAL VARIABLES.....	44
A. RESULTS.....	44
B. DISCUSSION.....	44
1. Corrosion Behavior in Deaerated Solutions.....	46
a. Effect of pH.....	46
b. Effect of Sulfite Ion Presence.....	47
c. Effect of Heat Treatment.....	48
2. Corrosion Behavior in Aerated Solutions.....	49
V. CONCLUSIONS.....	51
REFERENCES.....	53
INITIAL DISTRIBUTION LIST.....	56



## I. INTRODUCTION

Today's technology demands the development of new materials offering better performance, increased reliability, and adherence to stringent property requirements. An important class of materials considered to fall into this category is composites. A composite is formed when two or more constituents are combined on a macroscopic scale. This new material is designed to combine the best features of each constituent by maximizing certain material properties. [Ref. 1]

Composite materials generally consist of a high strength or high modulus reinforcement combined with a bulk material, called the matrix. The reinforcement, which may be in the shape of particles, whiskers, or fibers, is the component that carries the major stresses and loads, while the matrix allows the transfer of these stresses and loads to the fiber. Composite materials can be divided into three broad groups based upon the matrix material: metal, ceramic, or plastic. [Ref. 2]

Metal matrix composites are promising materials for use in structural or dynamic applications because they can take advantage of the many superior material properties of both the matrix and the reinforcement. These advantages include the combination of the following properties: [Ref. 2]

- High specific strength and modulus
- High toughness and impact properties
- High electrical and thermal conductivity
- Excellent reproducibility of properties

A particular metal matrix composite (MMC) widely used today consists of an aluminum matrix and a graphite fiber reinforcement. Aluminum and its alloys are of interest to the industrial and scientific communities because of their strength and formability combined with low density, their good thermal and electrical conductivities, and their

ability to resist corrosion [Ref. 3]. Graphite fibers possess both a high modulus of elasticity and a high thermal conductivity. The proper combination of aluminum and graphite to form a MMC should produce a new material which has high stiffness and strength, good ductility, and high thermal conductivity. [Ref. 4]

The Naval Weapons Support Center, Crane, Indiana has chosen a 6063 aluminum alloy reinforced with 27 volume percent P130-x continuous graphite fibers as a potential candidate for use in electronic module frames because of its low density, high stiffness, and high thermal conductivity. The combination of these key properties is necessary as weight, vibration reduction, and heat removal are all potentially limiting design factors. In his master's thesis [Ref. 4], LT King proposed composite elastic modulus and thermal conductivity values determined from the rule of mixtures. The analysis indicates that by forming this composite monolithic 6063 aluminum's elastic modulus is raised more than threefold and its thermal conductivity by almost twofold. These results indicate that combining 6063 aluminum and P130-x graphite fibers gives a composite capable of meeting the high stiffness and thermal conductivity demands of advanced electronic module frames.

In addition to processing, performance, and material property studies, an evaluation of this MMCs resistance to corrosive marine environments is necessary.

## **A. CORROSION OF ALUMINUM ALLOYS--MECHANISMS AND BEHAVIOR**

The thermodynamic stability of aluminum in water is commonly expressed by the potential-pH diagram which was devised by Pourbaix and is shown in Fig. 1 [Ref. 5,6]. This diagram delineates regions in which corrosion of aluminum is likely to occur. Aluminum forms a passive oxide barrier or exhibits immunity in the other regions. For example, deviations in pH above or below the range of 4 to 9 results in a shift from a

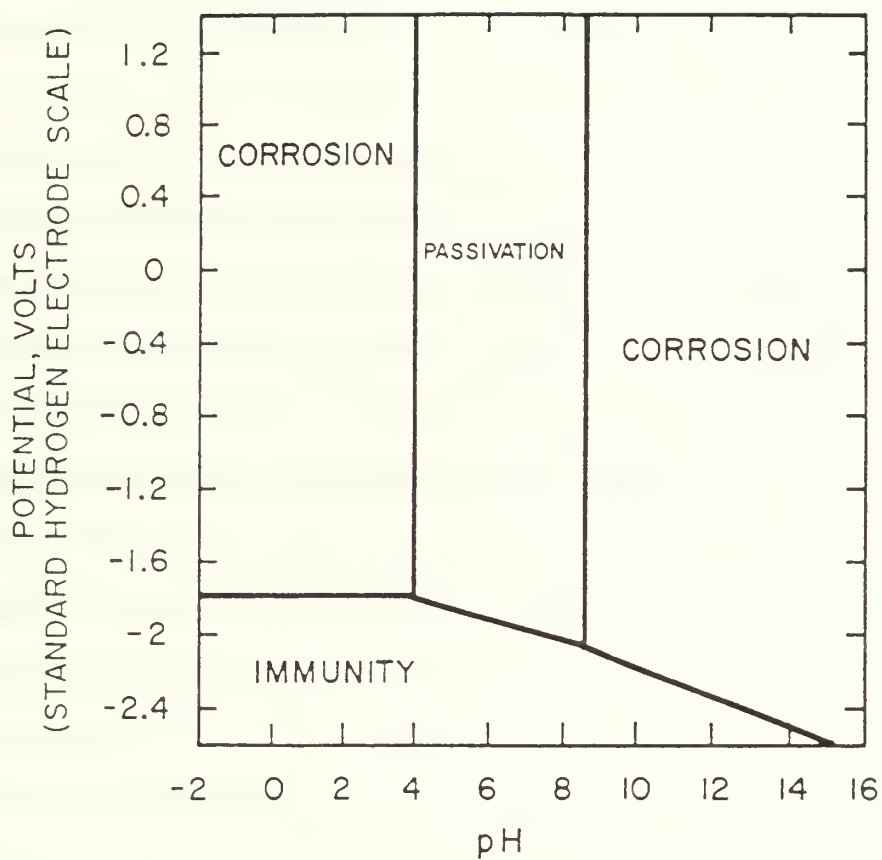


Figure 1: Pourbaix diagram for aluminum in H<sub>2</sub>O at 25 degrees Celsius.

regime in which pitting will be the predominate mode of corrosion to one in which general corrosion predominates.

When exposed to the atmosphere, aluminum immediately forms an adherent and 'complete' oxide layer. Upon immersion in water, this film grows to some equilibrium thickness depending on several factors which include temperature and pH. In environments of near neutral pH, defects in the oxide film may lead to a pitting mode of corrosion. Aluminum is very susceptible to this form of attack, but at the same time shows good resistance to general corrosion.

Pitting is not only the most common form of attack in aluminum, but it is also the most insidious. Preferential pitting attack occurs at defects in the oxide film usually due to surface inclusions. Inside the pit, aluminum ions are hydrolyzed raising the acidity within the pit and causing further pit propagation. As this process proceeds a cap of various aluminum oxides and hydroxides forms over the pit eventually blocking its operation [Ref. 6]. The chloride ion and other halides play a significant role in this process [Ref. 7].

In marine environments, the primary corrosive ingredient is chloride ion. Sea water contains various salts, in addition to NaCl, amounting to approximately 3.5% by weight of sea water. In order to simplify and standardize laboratory experiments in which sea water testing is to be done, an aqueous 3.5% NaCl solution is often used. This is necessary to help eliminate all the possible complicating variables introduced by the vast number of ionic species present in sea water. [Ref. 4]

Besides those species which are naturally occurring in sea water, some man-made species are also of concern. For example, ships use fuels containing varying amounts of sulfur. During combustion, sulfur in the fuels forms sulfur dioxide ( $\text{SO}_2$ ) and sulfur trioxide ( $\text{SO}_3$ ). When these mix with the moist environment they form sulfuric and

sulfurous acids. Of these, sulfurous acid is the most serious corrosive material and can exist in a variety of concentrations depending upon fuel sulfur content, power setting, and other factors. [Ref. 8]

Many researchers [Ref. 9,10,11,12] have studied the interaction between passive aluminum films, ions present in solution, and pitting susceptibility. While a mechanism describing the propagation of pitting has been generally accepted, there exists no clear understanding of how pitting is initiated. Isaacs [Ref. 9] states: "The processes which occur in the passive layer which are directly responsible for its breakdown and the onset of localized corrosion are at present unclear." He goes on to suggest some possible causes as: adsorption, penetration, passive film solubility, perturbation events, and vacancy clustering. The apparent bottom line is that two things are necessary to initiate pitting: (1) an aggressive anion and (2) particular heterogeneities in the metal. Isaacs concluded that in aluminum breakdown and repassivation occur at the same point in the passive film. Tan and Chin [Ref. 10] determined that anodic polarization of 6061-T6 aluminum in neutral sodium sulfate solutions resulted in passivation of the material with no pitting. But, with the gradual addition of chloride ion passivity was destroyed. Above about 100 ppm chloride ion added pits began to form and increased in size and density with increasing chloride ion concentration.

In their background study, Elboudjaini et. al. [Ref. 11] referenced various research discussing the effect that chloride and sulfate ions have on passive oxide film stability. This research indicated that the ionic resistance of the passive oxide film is lowered when chloride ions are present and get included at certain selected locations in the film. Sulfate ions, on the other hand, do not get included in the film and, as a result, there is no harmful effect on film resistance. Other research [Ref. 12] has shown that immersion of many aluminum alloys, including alloy 6061, in 1000 ppm cerium chloride for one week

markedly improves their resistance to localized corrosion. A conclusion of this research was that the use of rare earth chlorides as media for passivation is worth evaluating.

Crevice and galvanic corrosion are two other important corrosion modes in aluminum alloys, in addition to general and pitting corrosion. The mechanism of crevice corrosion is the same as that for pitting, in general. It is autocatalytic in nature, occurs in very localized regions, and requires mobility differences between ionic species to operate. In sodium chloride solutions, aluminum in contact with most other metals, will corrode preferentially. Aluminum becomes the anode and cathodically protects the metal connected to it. The degree to which aluminum corrodes when coupled to a more cathodic metal depends on the area ratio of the couple, the degree to which the aluminum is polarized, and the electrolyte. If aluminum must be coupled to a more cathodic metal, the most desirable arrangement would be to have a large aluminum to small cathode area ratio. When coupled to aluminum, some metals will polarize the aluminum sufficiently to cause it to exceed its pitting potential. Galvanic corrosion will be accelerated in electrolytes containing halide salts, aeration, and plenty of cathodic reactant. [Ref. 5]

## **B . CORROSION MECHANISMS AND BEHAVIOR OF MMC'S**

Because of their dual nature, metal matrix composites are susceptible to three adverse processes: galvanic coupling of the matrix and the reinforcement, crevice attack at the matrix/reinforcement interface, and preferred localized attack at structural and compositional inhomogeneities within the metal matrix [Ref. 13].

Some knowledge of the various MMC fabrication techniques and the problems encountered in them is necessary before considering possible corrosion processes in MMCs. For instance, fibers are sometimes reactive or nonwetting [Ref. 14] with the molten matrix material and must be coated to make the fibers wettable and limit fiber reactivity. If this coating is imperfect, the effect on material properties may be deleterious.

Carbides, oxides, or intermetallics may form at matrix/reinforcement interfaces during high temperature processing. Vastly different thermal expansion coefficients between the matrix and the reinforcement can result in large thermal residual stresses upon cooling [Ref. 4]. These and other processing artifacts can result in additional corrosion beyond that listed above and due to the simple combination of matrix and reinforcement.

Traditional descriptions of corrosion behavior include material weight loss, thickness reduction, and pit depth [Ref. 15]. Some weight loss experiments [Ref. 15,16] done on MMCs indicate that this approach may need some revision. In some cases, especially with graphite/aluminum MMCs, these researchers saw initial composite weight **gain** from the oxide formed and trapped during the corrosion process. As a result, tests which give weight loss results are potentially inappropriate and should be reserved for qualitative judgements only.

Vassilaros et. al. [Ref. 15] performed a qualitative study of the corrosion behavior of two different types of VSB-32 graphite 6061 aluminum MMCs. They found that when excessive exposure to a marine environment was allowed, pitting initiated on the surface foils and propagated to the graphite/aluminum interfaces. The aluminum corrosion product formed in the pit blistered the MMC. In their marine environment exposure studies, edge protection was used on some samples in order to elucidate various corrosion behaviors. This protection consisted of a coating applied only on surfaces with both matrix and reinforcement exposed. The samples without edge protection experienced much more severe corrosion than those with edge protection.

Additional qualitative studies of the corrosion behavior of MMCs have been conducted. Pfeifer [Ref. 16] studied the marine atmospheric corrosion of Thornel-50 graphite fiber 201 and 202 aluminum MMCs. He found that corrosion, once initiated, continued preferentially along foil interfaces and between wires. This type of attack was

more rapid than attack along the fiber/matrix interfaces. Aylor and Kain [Ref. 17] tested various silicon carbide and graphite/aluminum MMCs in marine environments. They found that for the graphite/aluminum composites tested, exposed edges resulted in blistering and exfoliation of the aluminum surface foils. The primary corrosion mode in silicon carbide/aluminum MMCs was pitting occurring at the matrix/reinforcement interfaces. In their status report on the corrosion of aluminum matrix composites, Metzger and Fishman [Ref. 18] reviewed past corrosion data and summarized their observations. They concluded that the types of corrosion seen in marine atmosphere studies was a result of imperfect consolidation of the composite including possible inadequate fiber wetting during infiltration of the fiber bundle. It appeared that well-bonded composites exhibited better corrosion resistance.

To date, the majority of MMC corrosion testing has been conducted in the laboratory under closely controlled conditions. More testing is necessary, however, because there are some questions that remain unanswered. The goals of the tests conducted thus far have been twofold. First, to describe how a composite will behave when environmental parameters are altered. And, second, to understand the principal modes of corrosion leading to degradation of a composite's material properties.

While some researchers have concluded that galvanic corrosion plays a major role in the accelerated corrosion of graphite/aluminum and graphite/magnesium MMCs, about an equal number have not. In her study of the corrosion behavior of graphite/magnesium MMCs, Trzaskoma [Ref. 19] determined that galvanic coupling plays an important role in the aqueous corrosion of graphite/magnesium composites. Vassilaros et. al. [Ref. 15] in their marine environment corrosion study of VSB-32 graphite 6061 aluminum composites, likewise determined that galvanic coupling was the dominant corrosion mechanism. Yet another group [Ref. 20] claimed that galvanic coupling in a graphite/aluminum composite

between the Thornel 50 graphite fibers and the 6061 aluminum alloy promoted crevice corrosion at the fiber/matrix interface.

These conclusions indicating the importance of galvanic coupling between the matrix and the reinforcement conflict with the conclusions of other researchers. For example, in two of their papers, Aylor and Moran [Ref. 21,22] concluded that galvanic corrosion between graphite fibers and the aluminum matrix is not the predominant reason for accelerated corrosion in graphite/aluminum composites. Instead, the accelerated attack is caused by some kind of segregation (or compound formation) at the fiber/matrix interfaces. In another study by Hihara and Latanision [Ref. 23] exfoliation of a P100 graphite fiber 6061 aluminum composite was shown to be more destructive than classical galvanic corrosion. The exfoliation was observed to be a result of the formation of pits in the diffusion bond regions caused by microstructural chloride containing zones.

Crevice attack at the matrix/reinforcement interface and preferred localized attack within the metal matrix have been found to be important in both graphite/aluminum composites and other MMCs. Sedriks et. al. [Ref. 24] used electrochemical techniques to study the corrosion behavior of boron/aluminum MMCs and found that crevice attack at the interface was the principle reason for the higher corrosion rate of the composite versus the unreinforced alloy. In the study mentioned above by Hihara and Latanision [Ref. 23], the graphite/aluminum composite was polarized to 2.0 Volts versus a saturated calomel electrode (SCE) in a deaerated 0.5M sodium sulfate solution at pH 7. Crevices were found to form under these conditions along the perimeters of the graphite fibers. The crevice formation was determined to be a result of the graphite oxidizing to carbon dioxide.

Preferred localized attack at microstructural inhomogeneities has been deemed important in certain cases. In the same research discussed above, Hihara and Latanision [Ref. 23] blame the titanium-boron chemical vapor deposition (Ti-B CVD) composite

fabrication process for allowing residual microstructural chlorides to become trapped within the diffusion bond regions. Severe pitting was observed to coincide with the diffusion bond regions causing the precursor wires to disbond. Trzaskoma et. al. [Ref. 25] studied the effects of silicon carbide on pit initiation susceptibility for three silicon carbide/aluminum alloy composite systems in sodium chloride solutions. They found that pitting potentials and hence the pitting susceptibilities of the composites were not much different from those of the unreinforced alloy. In a more recent study, Trzaskoma [Ref. 26] determined that pits initiated at secondary particles within the matrix of a silicon carbide/5456 aluminum alloy. It was shown that these particles were intermetallic phases composed of alloying elements Mg, Cr, Mn, Fe, and Al.

### **C. RESEARCH OBJECTIVES AND OVERVIEW**

There were two primary objectives in this investigation of the aqueous corrosion of a P-130x graphite/6063 aluminum composite. First, to characterize the composite's corrosion behavior in an aqueous 3.5% sodium chloride solution while varying solution pH and aeration, matrix heat treatment, and the presence of sulfite ion. And second, to understand the fundamental mechanism or mechanisms of corrosion in this composite in both 3.5% sodium chloride and 5.0% sodium sulfate solutions. Both electrochemical and immersion tests were employed in this research.

The experimental materials and procedures used will be detailed before discussing the results of both the mechanism and behavior studies.

## II. EXPERIMENTAL MATERIALS AND PROCEDURE

### A. MATERIALS

The P-130x graphite fibers used both in the fabrication of the composite and in this research as electrode material for galvanic corrosion testing were obtained from Amoco Performance Products, Richfield, Connecticut. The fibers are experimental as the 'x' in P-130x indicates and are roughly 10-12 mm in diameter. They are continuous throughout the composite, but their cross-sectional shape, while nominally circular, is predominantly irregular due to difficulty in fabrication. The fibers obtained directly from Amoco came in a spool-wound 2000 fiber tow, with no twist.

The control monolithic 6063 aluminum used in this research was obtained from ALCOA as extruded angle stock in the -T1 (overaged) temper.

The composite was fabricated by DWA Composites, Chatsworth, California. Fabrication was by a proprietary method which involved coating the 2000 fiber tow using the Titanium Boron chemical vapor deposition (Ti-B CVD) method and infiltrating the coated fiber tow with molten 6063 aluminum to form precursor wires. The precursor wires were then layed out in alternating 0° and 90° biases between two layers of 6063 aluminum foils. This "sandwich" was then diffusion bonded to form the final 0-90 cross-plyed continuous fiber composite. The as-received composite was determined to be in the overaged condition. Figure 2 shows an optical micrograph of a composite cross-section. Between the two surface foils (top and bottom) are eight alternating layers of graphite fiber/6063 aluminum diffusion bonded precursor wires. The only exception in this composite is that the center two (of the eight alternating) layers of precursor wires are

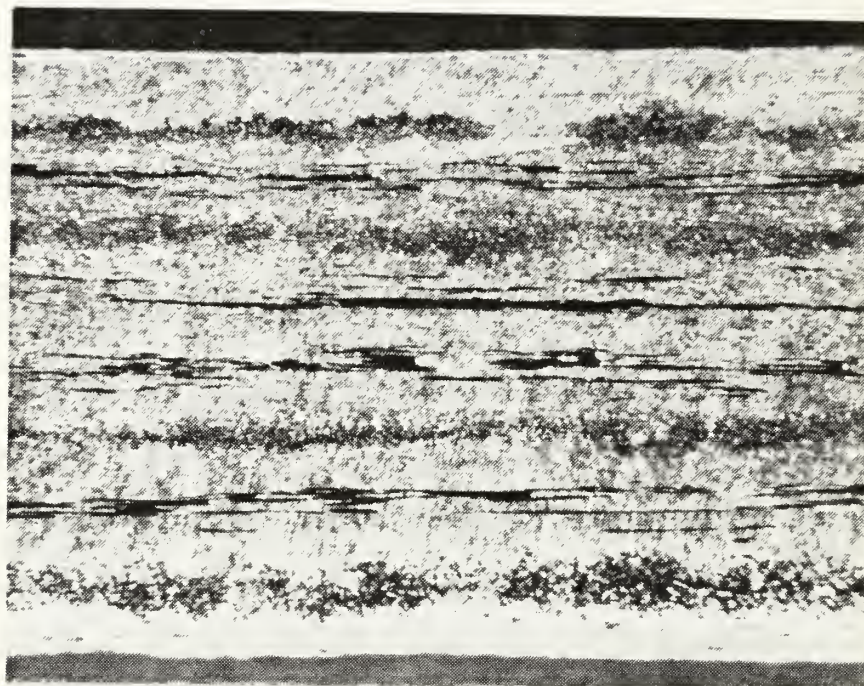


Figure 2: Optical micrograph of a composite edge revealing longitudinal and transverse fiber layers and composite surface foils (top and bottom). (50X)

aligned parallel to each other. The finished product was supplied in sheets 0.15 m long, and 0.0015 m thick.

## **B . SAMPLE PREPARATION AND ELECTRODE FABRICATION**

### **1. Composite and 6063 Monolithic Aluminum**

Specimens for most of the electrochemical tests were cut into disks 0.015 m in diameter. This was accomplished for both the monolith and the composite by electric discharge machining using a brass electrode. The monolithic metal electrodes used in the galvanic corrosion runs were machined to a 0.0151 m by 0.020 m by 0.003 m rectangular slab, and then tapped to accept the specimen holder rod on one of the 0.0151 m by 0.003 m faces. Immersion tests were conducted on coupons of composite material measuring 0.014 meters long by 0.007 meters wide by 0.0015 meters thick.

Immediately prior to all experiments, the monolith and composite specimens were wet sanded to 600 grit on SiC paper. With the composite, this was done most carefully, to avoid perforation of the surface foil. The specimens were then rinsed in tap water followed by a distilled water rinse, an ethanol rinse, and then dried under a hot air gun. Certain polarization and immersion tests required that the exposed specimen surface be polished. In all cases the specimens used in these tests were first polished on a 6  $\mu\text{m}$  diamond paste wheel (after 600 grit SiC paper) followed by a 3  $\mu\text{m}$  and 1  $\mu\text{m}$  diamond paste polishing.

As part of the mechanism study, samples were viewed in the SEM and/or light microscope after testing. The procedure for cleaning these samples was as follows. First, a rubber stopper was rubbed back and forth (under running tap water) across the exposed surface to remove the majority of the corrosion products. Second, the samples were rinsed in distilled water and ethanol and then dried under a hot air gun. Additional corrosion products were removed by stirring the sample in a beaker of 70% nitric acid for about two

to three minutes according to NACE Standard TM-01-69 [Ref. 27]. Finally, the samples were again rinsed in tap water, then distilled water and ultrasonically cleaned in ethanol.

## **2. Graphite Fiber Electrodes**

Graphite fiber electrodes were required as the second working electrode in the galvanic corrosion experiments along with the monolithic aluminum slabs. They were constructed by soldering to an electrical connector both a length of graphite fiber tow and an insulated copper wire. The wire, with attached length of graphite fiber tow, was then pulled through a 0.10 m length of Vycor tubing until about a 0.015 m length of fibers were left protruding from the opposite end of the tube. The end of the tube with graphite fibers left protruding was plugged with a slow-curing epoxy. At the other end of the tube, some of the excess wire was secured to the outside top of the tube with electrical tape to prevent any movement of the soldered junction. To complete the assembly, the free end of the wire and the wire end of the glass tube were fed through the hole in a rubber stopper. The schematic drawing of a similar graphite electrode assembly can be found in LT King's master thesis [Ref. 4].

## **C. EXPERIMENTAL**

### **1. Data Acquisition Equipment**

An EG&G Princeton Applied Research (PAR) Corporation Model 351 Corrosion Measurement System was used in all electrochemical tests. This system was comprised of a PAR Model 1000 System Processor connected through a parallel interface to a single PAR Model 273 Potentiostat/Galvanostat. The PAR Model K47 Corrosion Cell was connected through an electrometer to the Model 273. The addition of an RE0093 Plotter rounded out the corrosion measurement system used here. A detailed description of the Model 351 Corrosion Measurement System can be found in the system's operating manual [Ref. 28].

## 2. Electrochemical Technique Parameters

There are eleven experimental techniques already set up and stored in the system software. These techniques may be used with the default parameters or may be modified by the operator. The techniques are listed in Reference 28, p. II-2. In this study, potentiodynamic, polarization resistance, galvanodynamic, galvanic corrosion, and corrosion potential techniques were used. The parameters chosen for each technique in this study will be summarized in the remainder of this section. The sample used in each test, except the galvanic corrosion runs and some polarization tests, was a disk held in the K105 flat specimen holder. This arrangement results in exactly  $0.0001 \text{ m}^2$  (or  $1 \text{ cm}^2$ ) of exposed surface area to the electrolyte. Exceptions to this sample geometry will be noted in the appropriate sections.

### *a. Corrosion Potential Test Parameters*

The only parameter controlled by the operator for this measurement is time. In general, 24 hours was a sufficient length of time to allow stabilization of the specimen's corrosion potential,  $E_{\text{corr}}$ . Curve smoothing choices available to the operator are: no smoothing, seven point smoothing, and 15 point smoothing. Seven point smoothing was used in all of the electrochemical tests.

### *b. Galvanic Corrosion Test Parameters*

The monolithic 6063 aluminum slabs presented a surface area of  $0.0008 \text{ m}^2$  to the electrolyte. As in the corrosion potential tests, 24 hours was usually a sufficient length of time for stabilization of the galvanic corrosion potential ( $E_{\text{galv}}$ ) to occur. The same was true for the stabilization of the galvanic corrosion current density,  $i_{\text{galv}}$ .

The graphite area fraction utilized in all galvanic corrosion runs was 0.40. This was accomplished by trimming excess fiber tow from the ends of the graphite fiber electrodes such that the appropriate exposed area ratio between graphite and monolithic

aluminum was established. Refer to Reference 4, Appendix C for detailed calculations leading to the necessary exposed length of graphite fiber.

### ***c. Galvanodynamic Test Parameters***

In the galvanodynamic test, a controlled current scan is performed on the specimen as specimen potential is measured. The galvanodynamic technique is set-up to allow reverse current scans enabling the operator to perform a procedure called cyclic galvanostaircase polarization. This procedure can be used to determine the repassivation potential,  $E_{rep}$ , of the sample. A comparison of  $E_{corr}$  and  $E_{rep}$  gives an indication of the material's susceptibility to pitting. A detailed description of the cyclic galvanostaircase polarization method can be found in References 4, 29, and 30.

In these tests, the current was stepped up to a maximum, and then stepped back down to zero amperes. The complete set of parameters used in these tests were:

- Initial I: 0  $\mu A$
- Vertex I: 120  $\mu A$
- Final I: 0  $\mu A$
- Initial Delay: 120 sec
- Threshold E: Pass
- Step I: 20  $\mu A$
- Smooth: Seven Point
- Step Time: 120 sec
- Measurements per Step: 120
- Area: 1  $cm^2$

### ***d. Polarization Resistance Test Parameters***

In this technique a controlled potential scan is performed on the specimen and the resulting current passing through the specimen is measured. Polarization resistance

plots developed from this method provide a means of determining the corrosion current density,  $i_{\text{corr}}$ . [Ref. 28: pp. VII 29-37]

The complete set of parameters used in these tests were:

- Initial E: 20 mV below  $E_{\text{corr}}$
- Final E: 20 mV above  $E_{\text{corr}}$
- Initial Delay: 3600 sec
- Scan Rate: 0.01 mV/sec
- Density: 2.7 g/cm<sup>3</sup>
- Area: 1 cm<sup>2</sup>
- Smooth: Seven Point
- IR Compensation: Disabled

#### *e. Potentiodynamic Test Parameters*

This technique was used entirely in support of the mechanism studies. The corrosion characteristics of monolithic 6063 aluminum, composite surface foils, and composite cross sections in various electrolytes were determined and compared using this technique. A vast amount of information can be obtained from the current-potential relationship developed with this method. This data can be used to determine  $E_{\text{corr}}$ ,  $i_{\text{corr}}$ , Tafel slopes, and other important electrochemical information.

All three sample types tested were polished to a 1  $\mu\text{m}$  finish using the sample preparation process outlined in part B of this chapter. The corrosion measurement system alignment for these tests was identical to that used in the other electrochemical tests. The flat specimen holder was also used in all tests. This presented no problem for the monolithic aluminum and composite surface foil samples, but for the composite cross section samples a modification to the sample's geometry was necessary. This was done by 'sandwiching' the composite between two hemispherical halves of Teflon and using slow-

cure epoxy to bond the sample between the two halves of Teflon. A disk-shaped specimen was obtained using this procedure. The exposed sample surface area in composite cross section tests was  $0.000016 \text{ m}^2$  (or  $0.16 \text{ cm}^2$ ).

The potential scans were all initiated at a potential sufficiently below the corrosion potential,  $E_{\text{corr}}$ , so that well-defined cathodic slopes could be generated. The complete set of parameters used in these tests were:

- Initial E: -500 mV versus  $E_{\text{corr}}$
- Final E: 1.5 V
- Initial Delay: 3600 sec
- Scan Rate: 0.01 mV/sec
- Smooth: Seven Point
- IR Compensation: Disabled

The three types of samples were each tested in both deaerated 3.5% sodium chloride and 5.0% sodium sulfate electrolytes. Argon gas was used to deaerate the solutions in all cases. Some of these tests were run to generate a full polarization curve, while other tests were stopped prematurely in order to investigate which regions were first attacked.

### 3. Behavior Study Tests

The electrolyte used in all behavior study tests conducted was a 3.5% sodium chloride solution. It was deaerated in all tests with Argon gas and buffered to either pH 4 or pH 8 with buffer capsules. Composite surface foils were exposed to the electrolyte during these tests and the matrix heat treatment was varied from a solutionized and quenched condition (-W) to a peak-aged condition (-T6) and to an overaged or as-received condition (-T1). In about one-half of the tests 100 ppm sulfite ion was added to the electrolyte.

$E_{corr}$ ,  $E_{rep}$ ,  $i_{corr}$ ,  $i_{galv}$ , and  $E_{galv}$  were measured for each combination of matrix heat treatment, pH, and presence or absence of sulfite ion. Analytical grade sodium chloride and 10 Megaohm-cm distilled water were used to prepare the solutions. Behavior study results and discussion are given in Chapter IV.

#### **4. Immersion Tests**

Solutions used in this testing were prepared in the same manner as described in the above section. Two types of tests were conducted in this portion of the mechanism study. The first type of test involved samples with only their surface foils exposed to the electrolyte, and in the second type of test, one polished composite edge and both surface foils were exposed. A thin run of slow-cure epoxy was applied to the composite edges which required protection.

Three immersion baths were prepared for the surface foil tests. All were aqueous 3.5% sodium chloride solutions. Two of the three were titrated to pH 4 with hydrochloric acid and the remaining bath was titrated to pH 8 with sodium hydroxide. To one of the pH 4 baths, 1000 ppm sulfite ion was added. The samples were immersed for 10 weeks, removed, and cleaned following the procedure outlined above prior to micrography.

Four samples with one polished edge exposed to the electrolyte were immersed in 3.5% sodium chloride and 5.0% sodium sulfate solutions. Immersion test run times were two and fourteen days. Two of the samples were immersed in the 3.5% sodium chloride electrolyte, one for two days and one for 14. The remaining two samples were immersed in 5.0% sodium sulfate, one for two days and one for 14. Exposed composite cross sections tested in this manner were also cleaned using the method outlined above.

### III. MECHANISM STUDY

#### A. RESULTS

##### 1. Immersion Tests

###### *a. Edge Protected Samples*

A low magnification (11X) micrograph of the three edge sealed immersion samples (after ten weeks immersion and before cleaning) can be seen in Figure 3. The top coupon was immersed in a 3.5% sodium chloride solution which was titrated to pH 8 with sodium hydroxide. The two bottom samples were also immersed in 3.5% sodium chloride, but they were titrated to pH 4 with hydrochloric acid. 1000 ppm sulfite ion was added to the electrolyte in which the bottom left sample was immersed.

Both samples immersed in the pH 4 electrolytes formed a thick, white, hydrated oxide film (probably hydrargillite,  $\text{Al}_2\text{O}_3 \cdot 3\text{H}_2\text{O}$ ) [Ref. 5] within one week versus relatively little formation on the sample immersed in the pH 8 electrolyte.

A closer look at the surface foil of the sample (after cleaning) which was immersed in the pH 8 electrolyte reveals no indication of pitting after ten weeks. Figure 4 shows a SEM micrograph (531X) of a general surface foil region. The appearance of the protective oxide film on this sample can be described as being porous.

The low magnification (11X) micrograph presented in Figure 5 was taken of the sample which was immersed in the pH 4 electrolyte containing no sulfite ion. This micrograph (taken after the sample was cleaned) reveals the relative location of pits which were observed under the SEM. A representative pit from this sample can be seen in Figure 6. Again, the oxide film on this sample in the area surrounding the pit has a porous appearance identical to that seen on the pH 8 specimen. The pits in this specimen's surface

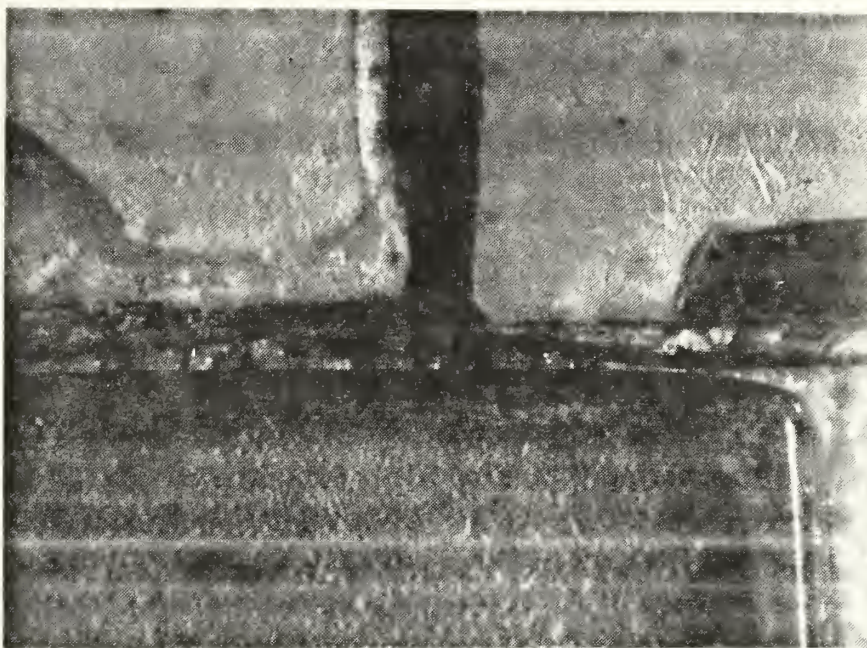


Figure 3: Low magnification micrograph (11X) of the three edge sealed immersion samples after ten weeks immersion (and before cleaning).

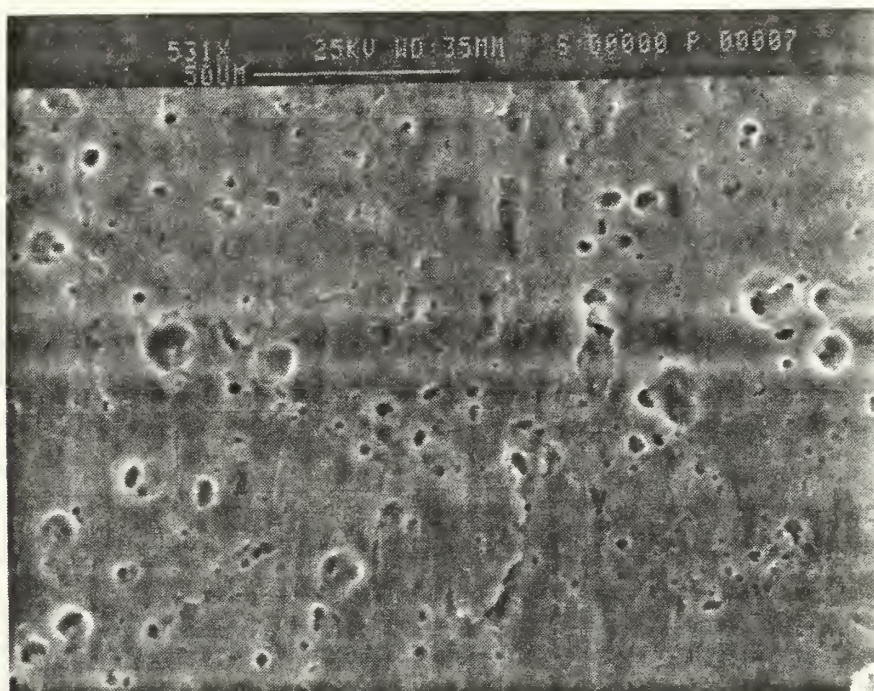


Figure 4: SEM micrograph of an edge protected sample immersed for ten weeks in 3.5% sodium chloride (titrated to pH 8). Taken after cleaning. (531X)

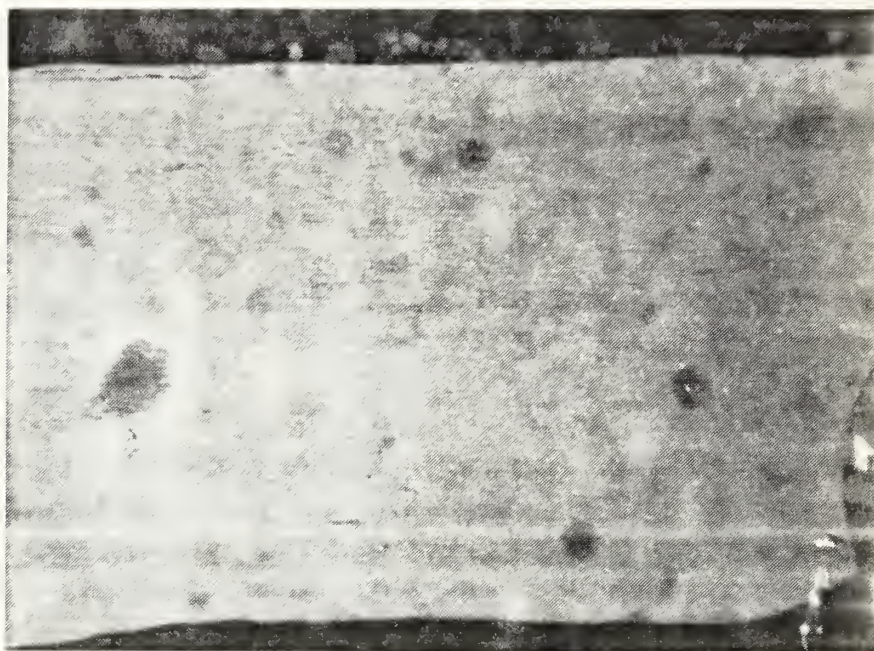


Figure 5: Stereomicroscope micrograph of an edge protected sample immersed for ten weeks in 3.5% sodium chloride (titrated to pH 4). Taken after cleaning. (11X)

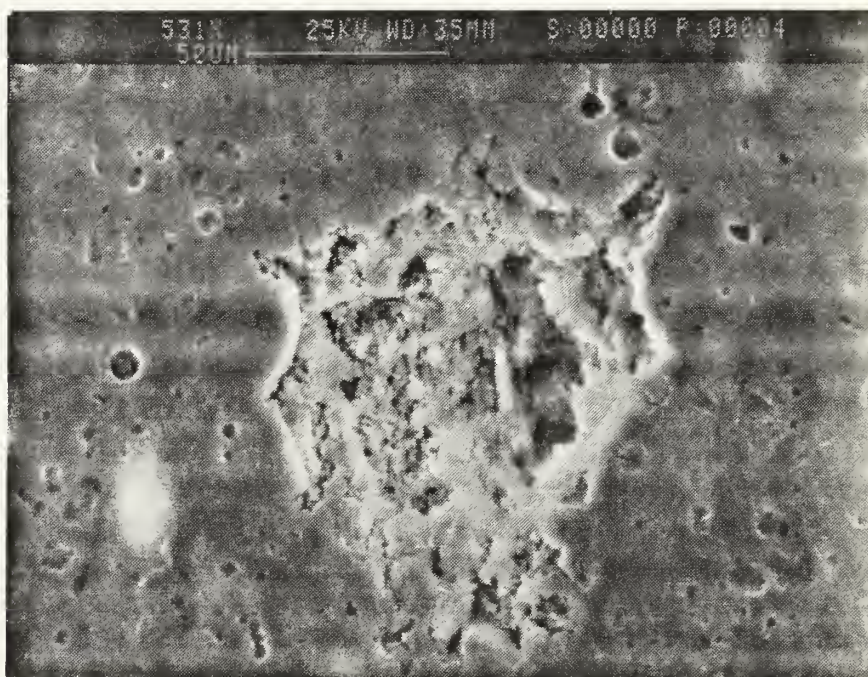


Figure 6: SEM micrograph of an edge protected sample immersed for ten weeks in 3.5% sodium chloride (titrated to pH 4). Taken after cleaning. (531X)

foil correspond to the widely spaced black spots (of varying diameter) seen in Figure 5. A region in the bottom of the pit shown in Figure 6 has been blown up and can be seen in Figure 7. Crystallographic facets are clearly visible in this SEM micrograph. Trzaskoma [Ref. 26] observed the same crystallographic behavior in pits formed on 5456 and 6061 aluminum alloys in sodium chloride solutions. This behavior is typical for aluminum and the faceting probably results from preferential etching of the {100} planes [Ref. 26].

Shown in Figure 8 is a low magnification (11X) micrograph of the sample which was immersed in the pH 4 electrolyte containing 1000 ppm sulfite ion (after cleaning). A comparison of Figure 8 to Figure 5 reveals that the addition of sulfite ion at pH 4 results in an increase in the surface foil pit density. The numerous, small black spots covering the surface of this specimen correspond to pits as seen under the SEM. Shown in Figure 9 is a representative pit from the surface of this specimen. A typical pit in this specimen measured 20 to 25 microns in diameter, compared to a diameter of 60 to 70 microns for a typical pit in the sample immersed in the pH 4 electrolyte containing no sulfite ion.

The protective oxide film in the region surrounding the pit shown in Figure 9 can be seen to have a dimpled appearance. This is in contrast to the porous appearance of the oxide layer formed on the surfaces of the pits immersed in both pH 4 and pH 8 electrolytes containing no sulfite. A high magnification blow up of a region in the bottom of the pit seen in Figure 9, can be seen in Figure 10. The same crystallographic faceting can be observed in this micrograph as in the micrograph in Figure 7.

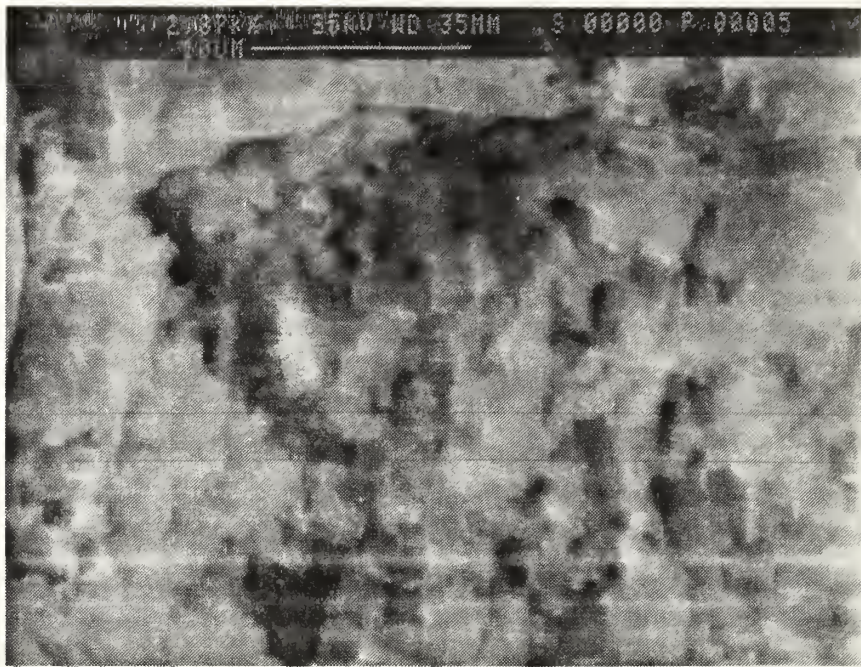


Figure 7: This SEM micrograph is a high magnification (2.87kX) blow-up of the bottom of the pit seen in Figure 6.

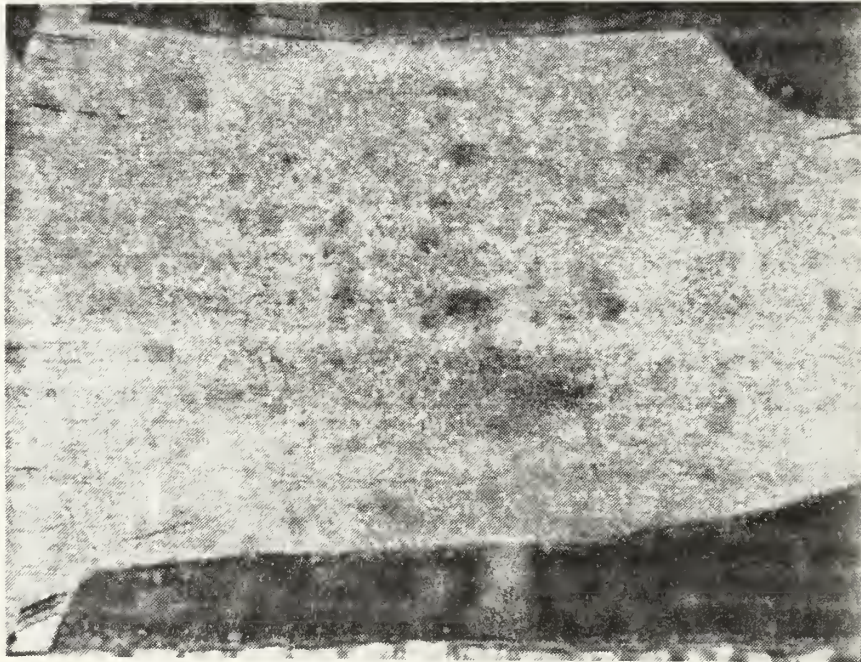


Figure 8: A stereomicroscope micrograph of an edge protected sample immersed for ten weeks in 3.5% sodium chloride (titrated to pH 4 and with 1000 ppm sulfite ion added). (11X)



Figure 9: SEM micrograph of the edge protected sample seen in Figure 8. (531X)

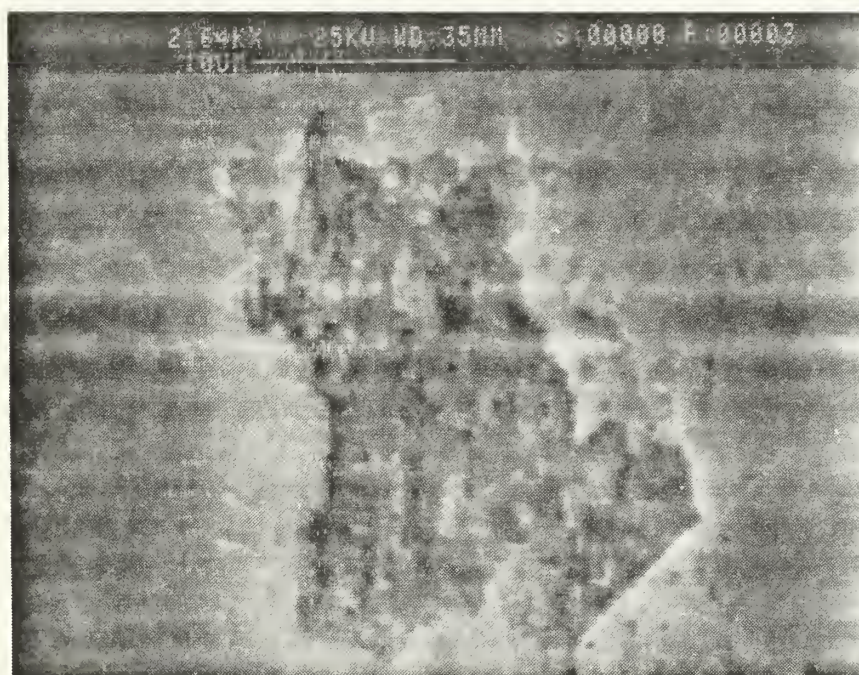


Figure 10: High magnification (2.64kX) SEM micrograph of the sample shown in Figures 8 and 9. This pit is a blow-up of the pit seen in Figure 9.

### *b. Non Edge Protected Samples*

After all four samples were cleaned using the method detailed in the procedures section, they were photographed under the SEM. Figure 11 is a micrograph of the sample immersed for two days in 3.5% sodium chloride. This top-down view clearly shows a region of accelerated dissolution adjacent to the graphite fibers (perpendicular to the plane of the page). The same sample surface, tilted about 45 degrees, can be seen in Figure 12. This orientation more clearly shows that the attack was not confined to just the regions immediately adjacent to the graphite fibers. But, rather, it shows that the attack is spread out over a wide area and into the aluminum matrix between fiber layers.

The sample immersed in 3.5% sodium chloride for fourteen days is presented in Figure 13 (also with 45 degrees of tilt). This micrograph indicates that if the attack were allowed to continue for an extended amount of time, the resulting matrix dissolution would leave only graphite fibers. Although the fibers are closely packed, it is evident that the aluminum that existed between the graphite fibers prior to immersion has been corroded away. Also evident, are fibers which were sheared off during the mechanical cleaning process. The fibers are protruding to such an extent from the matrix that less closely packed fibers were sheared off at their bases.

In Figures 14 and 15 are two more micrographs of composite edges. These two samples were immersed in 5.0% sodium sulfate. The sample in Figure 14 was immersed for two days and the one seen in Figure 15 for fourteen days. Again, both samples were tilted to allow clear interpretation of the extent of corrosive attack.

Looking at the sample immersed in sodium sulfate solution for two days, it can be seen that the fibers are extending above the matrix surface but to a lesser degree than in the sample which was immersed for two days in 3.5% sodium chloride (Figure 12).

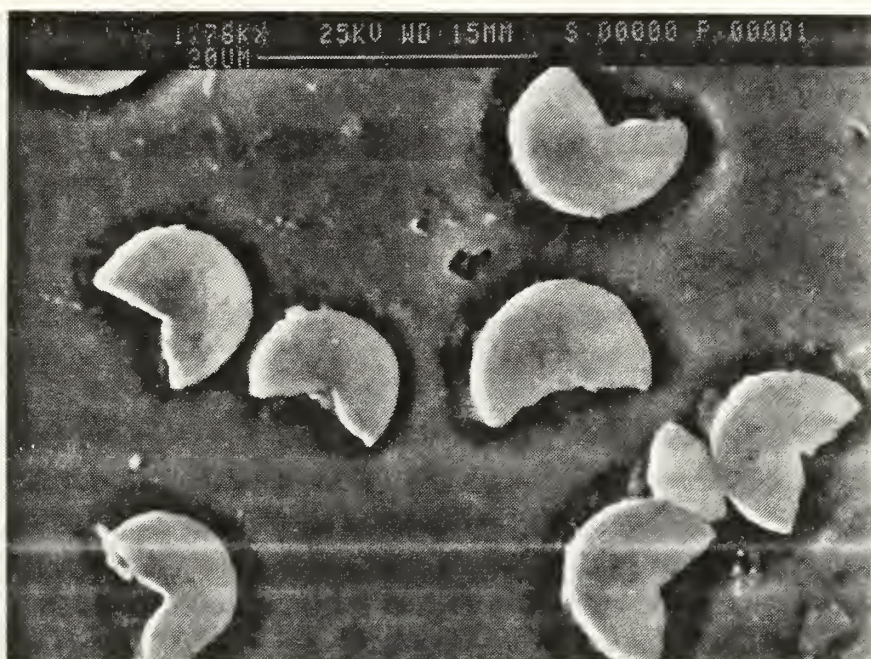


Figure 11: High magnification (1.78kX) SEM micrograph of the edge (unprotected) of a composite sample immersed in 3.5% sodium chloride for two days.

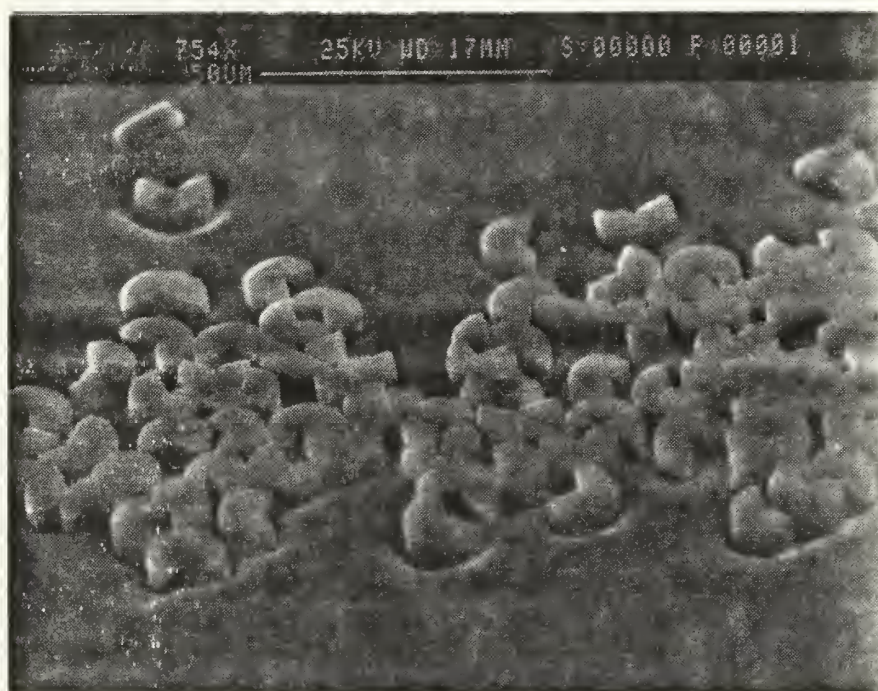


Figure 12: SEM micrograph of the same sample surface shown in Figure 11. This micrograph was taken with the sample tilted 45 degrees. (754X)

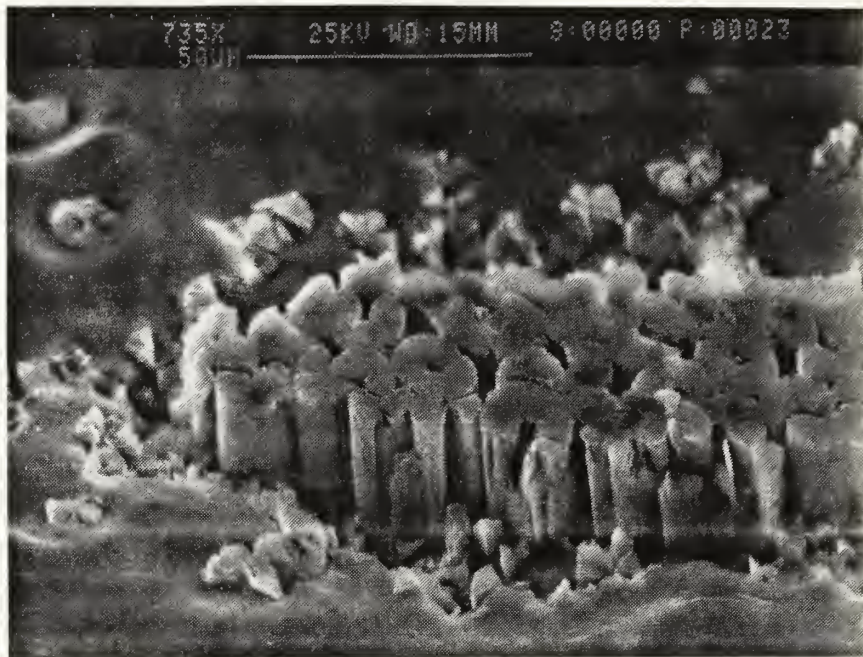


Figure 13: SEM micrograph of an unprotected edge sample immersed in 3.5% sodium chloride for 14 days. The sample is tilted 45 degrees. (735X)

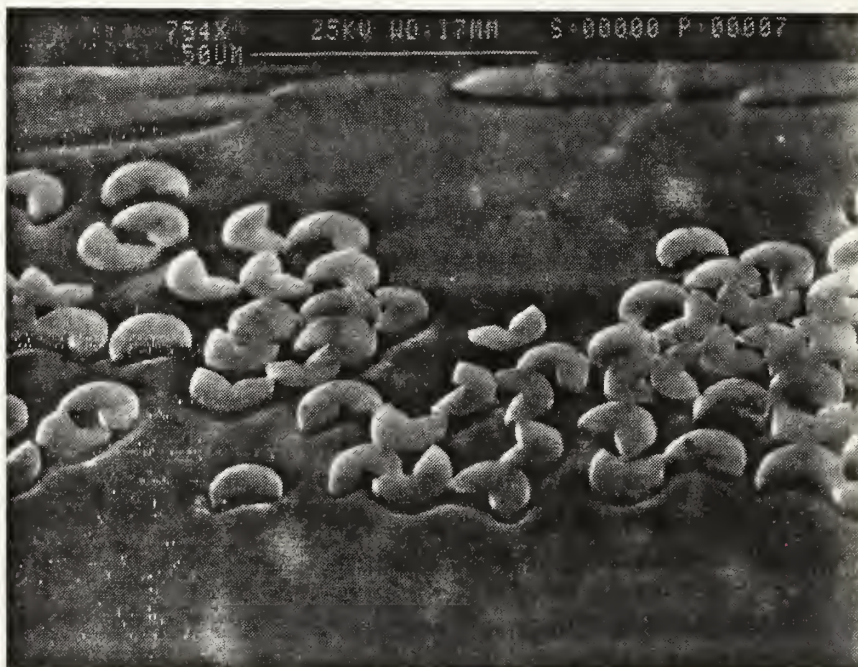


Figure 14: SEM micrograph of an unprotected edge sample immersed in 5.0% sodium sulfate for two days. The sample is tilted 45 degrees. (769X)

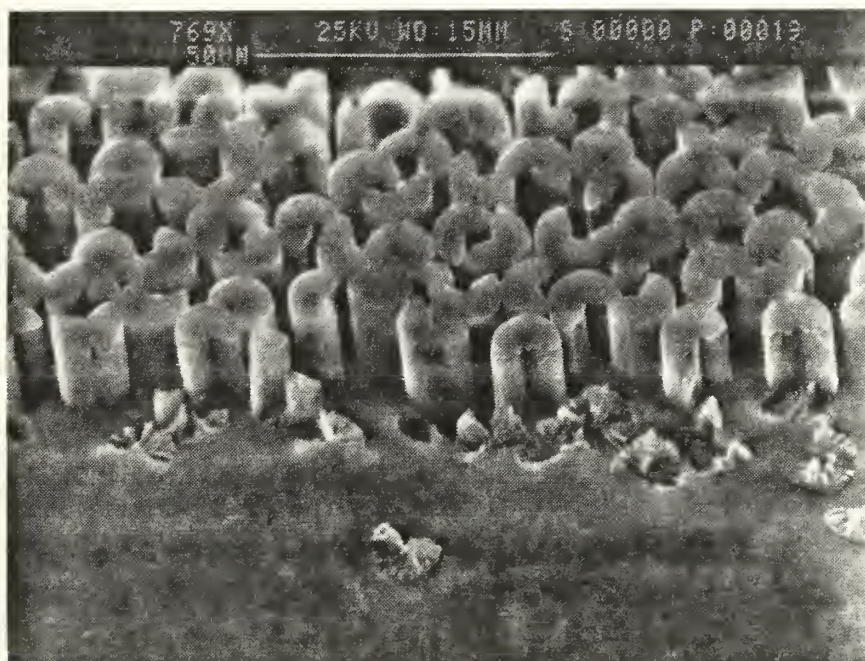


Figure 15: SEM micrograph of an unprotected edge sample immersed in 5.0% sodium sulfate for 14 days. The sample is tilted 45 degrees. (769X)

Another noticeable feature about the corrosive attack on the surface of this sample is that there is a slight dip in matrix elevation in the regions immediately adjacent to the fibers.

After fourteen days, the sample shown in Figure 15 has suffered severe corrosive attack of the same order as that sustained by the sample immersed for fourteen days in sodium chloride. It does appear, however, that the extent of attack is slightly greater in the sample immersed in sodium chloride. Another result common to all four edge exposed immersion samples is the fact that graphite fiber diameters remained constant no matter what the exposure length.

## 2. Electrochemical Test Results

### *a. Polarization Test Plots*

Of the six full polarization tests conducted, the results of four are shown in Figures 16 and 17. Table 1 gives the pertinent electrochemical data derived from these polarization plots. The data from two other plots, which are not shown, is also included in the table.

There are many key points which can be generated from these plots and from Table 1. First, the shape of the anodic regions in the four plots indicates that sodium sulfate is passivating to the monolith and the composite cross section while sodium chloride is not. The Tafel slopes,  $\beta_a$  and  $\beta_c$ , were determined from the anodic and cathodic polarization legs of the respective plots and entered in Table 1. A comparison of these slopes also indicates that sodium chloride is a far more aggressive electrolyte than sodium sulfate. For instance,  $\beta_a$  increases from 19.5 mV/decade for the monolith in sodium chloride to 492 mV/decade for the monolith in sodium sulfate.

Another key point is that the corrosion current density ( $i_{\text{corr}}$ ), and therefore the corrosion rate, is greater for the composite cross section than for the composite surface foil or the monolith in both sodium chloride and sodium sulfate electrolytes. Also,  $i_{\text{corr}}$  for

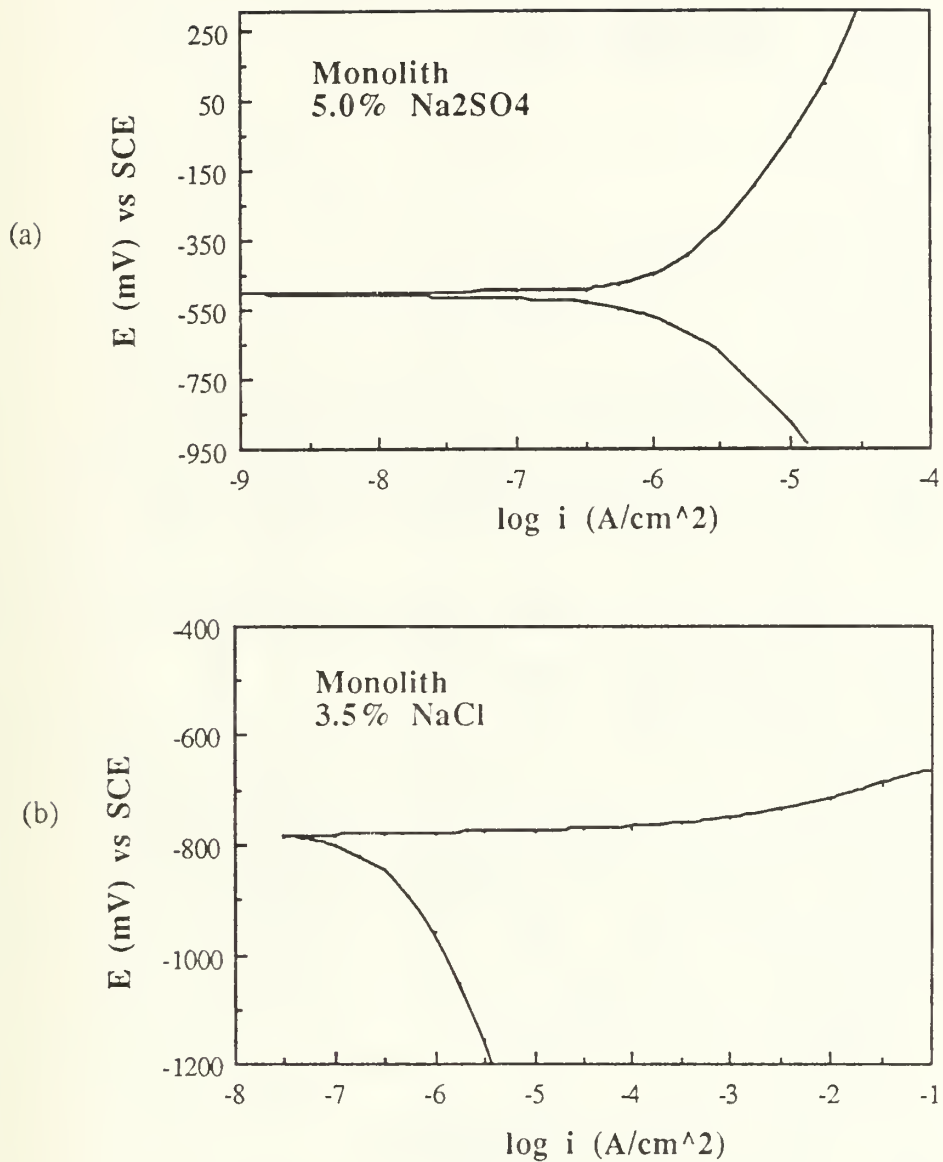


Figure 16: (a) Polarization curve for 6063 aluminum monolith in 5.0% sodium sulfate.  
(b) Polarization curve for 6063 aluminum monolith in 3.5% sodium chloride.

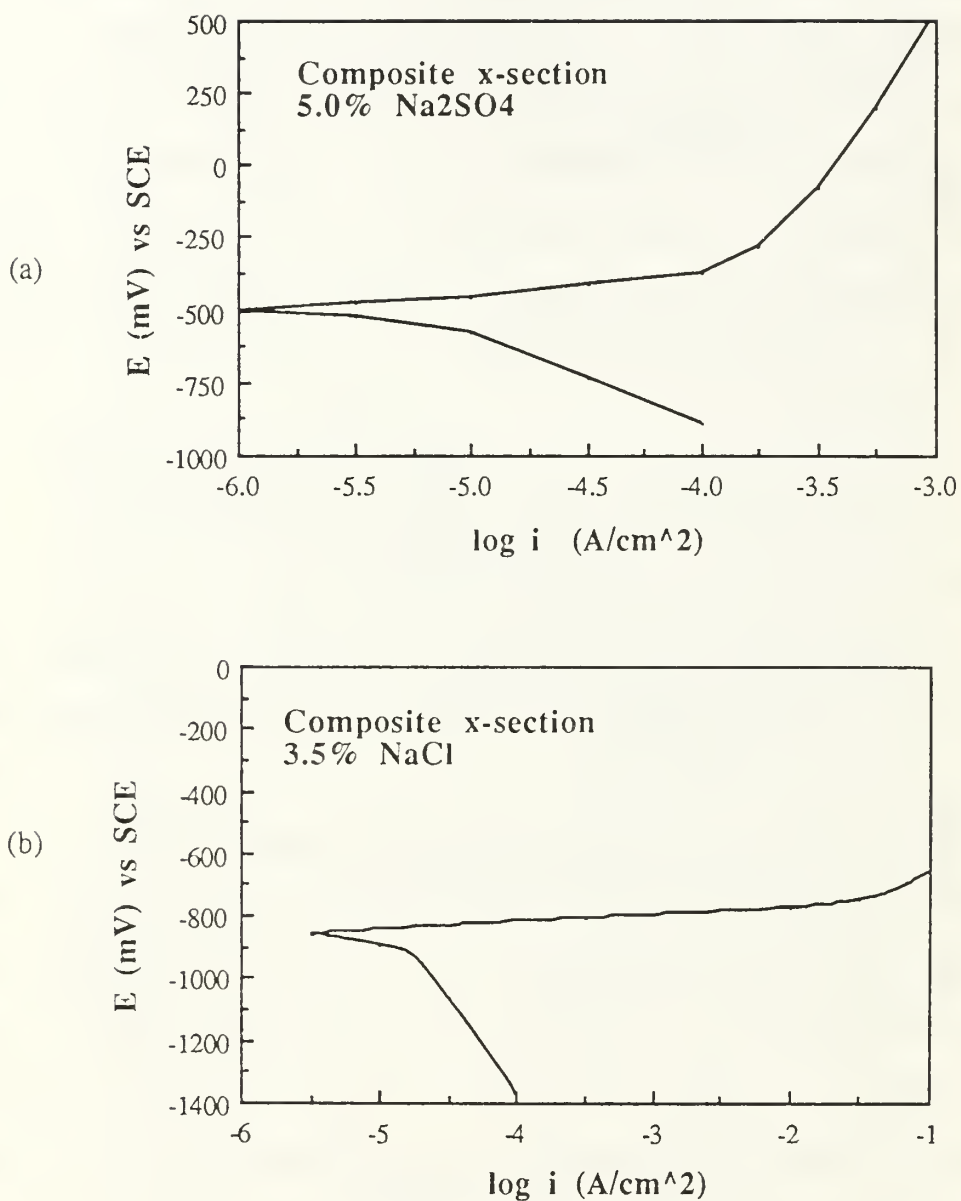


Figure 17: (a) Polarization curve for the composite cross section in 5.0% sodium sulfate.  
(b) Polarization curve for the composite cross section in 3.5% sodium chloride.

TABLE I  
SUMMARY OF POLARIZATION TEST RESULTS

Material/Exposed Surface/Electrolyte	$\beta_a$ , mV/dec	$\beta_c$ , mV/dec	$i_o$ , $\mu\text{A}/\text{cm}^2$	$i_{\text{corr}}$ , $\mu\text{A}/\text{cm}^2$	$E_{\text{corr}}$ , mV
Composite/cross section/NaCl	15.5	615	1.4	13.2	-828
Composite/surface foil/NaCl	22.0	334	0.010	0.37	-780
Composite/cross section/Na <sub>2</sub> SO <sub>4</sub>	88.0	340	1.1	5.3	-460
Composite/surface foil/Na <sub>2</sub> SO <sub>4</sub>	858	568	0.63	0.71	-284
Monolith / NaCl	19.5	420	0.018	0.37	-779
Monolith / Na <sub>2</sub> SO <sub>4</sub>	492	426	0.30	1.2	-510

the cross section in sodium chloride is approximately two and one-half times greater than in sodium sulfate (Table 1). The remaining  $i_{\text{corr}}$ 's were found to be very close to each other. The corrosion potential values found in tests conducted in the sodium sulfate electrolyte are, in general, considerably noble to those found in tests conducted in the sodium chloride electrolyte.

The exchange current density ( $i_0$ ) is yet another important electrochemical parameter which can be generated from these tests. The  $i_0$  values given in Table 1 are for the hydrogen reduction reaction. From Table 1, it can be seen that the  $i_0$ 's determined from the composite surface foil and monolith polarization tests in sodium chloride are on the order of  $10^{-8}$  A/cm<sup>2</sup>. This is about 2 orders of magnitude less than the remaining  $i_0$  values. For instance,  $i_0$  found for the composite surface foil in sodium chloride is about 140 times less than the  $i_0$  found for the composite cross section in sodium chloride. The only variable changed between these two tests was that graphite fibers were exposed simultaneously with matrix in the cross section test.

This last result will be considered in the mechanism discussion section along with a superposition of the four polarization plots.

#### ***b . Polarization Test Micrographs***

Figure 18 shows a SEM micrograph of a composite pit profile which formed during anodic polarization of the composite's surface foil in 3.5% sodium chloride. Upon close examination, it can be seen that the matrix metal within regions of high fiber density is attacked preferentially. Also apparent, is the fact that once the pit has propagated to the underlying fiber layer, matrix dissolution proceeds rapidly along the longitudinal fiber direction. These results suggest either galvanic coupling or localized crevice corrosion at the interface and in regions of high fiber packing.

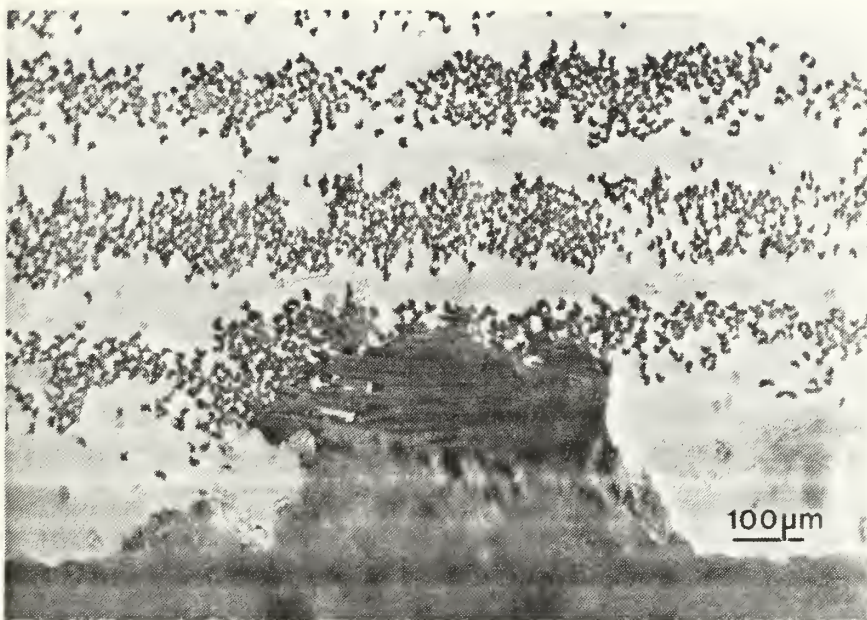


Figure 18: SEM micrograph of a composite pit profile formed during anodic polarization of the composite's surface foil in a 3.5% sodium chloride solution.

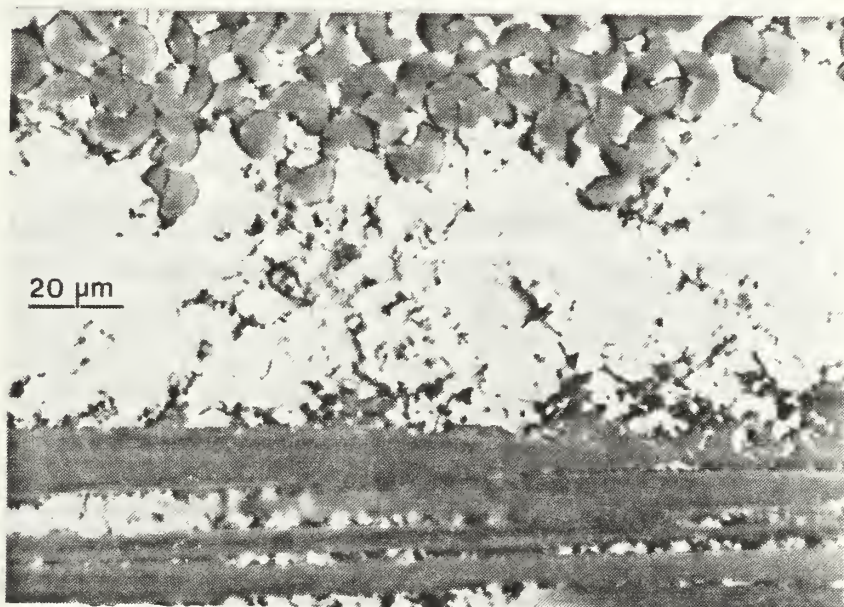


Figure 19: SEM micrograph of a composite cross section lightly polarized in a 3.5% sodium chloride solution.

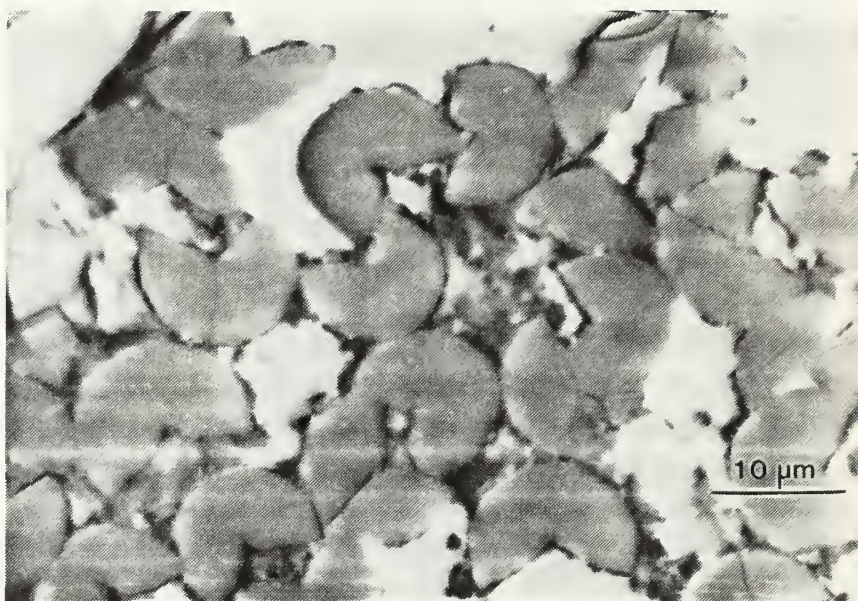


Figure 20: SEM micrograph of the same sample seen in Figure 19, but at a higher magnification.

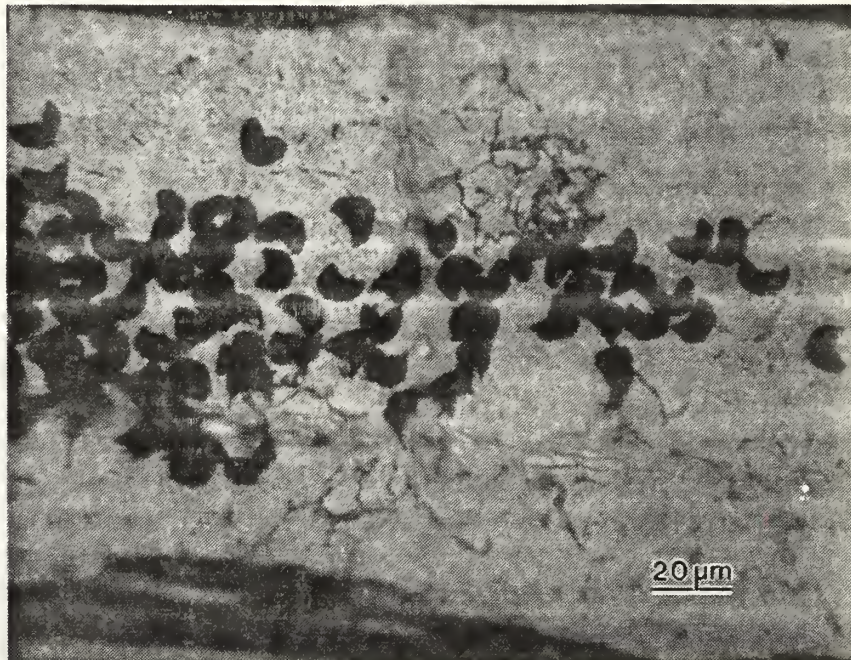


Figure 21: Optical micrograph of a composite cross section etched in Keller's Reagent.

SEM micrographs were also taken of a composite cross section which was anodically polarized (lightly) in 3.5% sodium chloride. These micrographs appear in Figures 19 and 20. They indicate that initial attack upon anodic polarization of composite cross sections occurs at fiber/matrix interfaces (Figure 20) and at localized regions between fiber layers (Figure 19). As shown in Figure 21, a composite cross section etched in Keller's Reagent shows localized attack similar to that observed in Figure 19. Apparently, upon anodic polarization, areas which are first attacked include all high energy regions--both at the fiber/matrix interface and at what are likely microstructural segregations at grain boundaries in the matrix between fiber layers.

## **B. MECHANISM DISCUSSION**

The task of establishing the principal corrosion mode(s) in aqueous environments for this MMC is complicated. Multiple corrosion modes are potentially superimposed or convoluted simultaneously. Therefore, a careful and comprehensive testing and evaluation scheme is necessary in order to decouple possibly overlapping effects. The corrosion modes most likely to be important in this MMC are galvanic coupling of the aluminum matrix with the graphite reinforcement, crevice attack at the fiber/matrix interface, and localized attack at structural and compositional inhomogeneities within the metal matrix [Ref. 13].

While these corrosion modes may arise due to the addition of graphite fibers to the aluminum matrix, the standard corrosion modes affecting aluminum alloys alone may also become important in this MMC. For example, if the edges of a composite coupon are all sealed, then only the surface foils will be exposed to the marine environment or electrolyte. In this case, general corrosion, pitting attack, stress corrosion cracking, galvanic corrosion, and corrosion fatigue of the surface foils would be the potential principal modes of corrosion in this composite unless, of course, the integrity of the surface foils is violated

[Ref. 5]. If this happens, then the corrosive nature of the underlying composite laminates must then be considered too.

Of the eight possible corrosion modes listed, two will be eliminated in the case of edge protected composite coupons before any discussion of results is undertaken. Stress corrosion cracking (SCC) can be eliminated as a potential mode of corrosion because, in the expected application of this composite, there will be no anticipated residual or applied stresses in the surface foils. This does not preclude the onset of SCC in underlying composite regions. Likewise, galvanic corrosion can be excluded as this composite is not expected to be physically connected to a more noble metal.

A summary of the edge protected immersion test results indicates that the 6063 surface foils are resistant to general corrosion but do experience some pitting under somewhat harsh conditions. After ten weeks immersion in a 3.5% sodium chloride solution, pitting had not initiated at pH 8, but did initiate at pH 4 with and without sulfite ions present. The presence of sulfite ion affected both pit size and pit density at pH 4 and also had an effect on the nature of the oxide film. The passive oxide film had a porous appearance in the absence of sulfite ion, while in the presence of sulfite ion its appearance was rough and dimply. Pit diameter at pH 4 was roughly three times greater when no sulfite ions were present, but pit density showed a corresponding decrease. Sulfite ions seem to stimulate pit initiation such that many pits form, but individual pit size remains small.

One possible explanation for this behavior involves the chemical nature of the sulfite ion and its interaction with the passive oxide film on aluminum. Sulfite ion is easily oxidizable to sulfate ion. Therefore, sulfite ion is a good reducing agent. Initially, the sulfite ion in the immersion test electrolyte will interact with the protective oxide film on aluminum, destabilizing it locally. This will result in many more pits initiating in a sulfite ion containing electrolyte versus one free of sulfite ion. But, after some time, as the sulfite

ion gets oxidized to sulfate ion the solution becomes even more passivating than it would have been with no sulfite ion addition in the first place. The result of this is that the many pits that were initiated are now passivating and slowing or possibly even stopping to grow entirely.

So, when constantly subjected to a harsh marine environment (chloride ion present, sulfite ion present, and low pH), composite surface foils are likely to experience attack in the form of pitting. If the surface foils are properly coated similar to the composite edges, then the pitting attack will probably be reduced. However, if the pitting is allowed to proceed to the underlying graphite fibers, additional corrosion processes (e.g., galvanic corrosion) become active. This could greatly accelerate the failure of this composite in use. Finally, if only the surface foils are exposed, then pitting attack is the predominant corrosion mode in harsh environments.

The immersion test results obtained from edge exposed composite samples shed considerable light on the process of determining this composite's principle mechanism of corrosion when graphite fibers are exposed simultaneously with the matrix. Of all the possible corrosion mechanisms listed at the outset of this section most may be eliminated as potentially operating on this composite in aqueous marine environments. For instance, crevice corrosion is an unlikely mechanism. Both sodium chloride and sodium sulfate immersion tests of samples with one edge not protected showed similar degrees of corrosion. This is contrary to what would be observed if crevice attack at the fiber/matrix interface were important. Crevice attack at the fiber/matrix interface in the sodium sulfate electrolyte is highly unlikely because no aggressive ion, such as chloride, is available to catalyze the process. Since the sodium sulfate induced matrix dissolution was comparable to that caused by the sodium chloride electrolyte, crevice attack is invalidated as a potentially important mechanism. It must be pointed out, however, that if crevice attack is

present in the sodium chloride electrolyte, then its severity is negligible compared to the principal corrosion mechanism.

If localized attack were the primary mechanism, then again, the vast majority of the matrix dissolution would have been concentrated in very small areas (either in the matrix between fiber layers or immediately adjacent to the fibers) and not spread out over the whole matrix surface as was observed in these tests. Specifically, interfacial attack, attack at compositional inhomogeneities, pitting, and graphite fiber oxidation can be ruled out as possible important mechanisms. The first three of these can be discounted as unimportant because of the widespread nature of the matrix dissolution. If these three do exist, then their effects are masked by a much more important mechanism. Graphite fiber oxidation can be ruled out because fiber diameter remained unchanged for the duration of the immersion testing.

The widespread matrix dissolution seen here is not a result of general corrosion. It was shown in the last section that general corrosion of the surface foils was rendered negligible by the formation of a protective oxide film over a large pH range. The same protective oxide film was not observed to form on the matrix in the unprotected edge tests. Also, in both two day immersion tests, the matrix immediately adjacent to the graphite fibers was observed to have undergone greater corrosion than elsewhere. This is another indication that general or uniform attack can be eliminated as important. Since the aluminum matrix material is no different than the composite surface foils, the only possible explanation for the widespread matrix attack is galvanic coupling between the graphite fibers and the aluminum matrix. This coupling effect hinders the aluminum's ability to form an oxide film and results in dissolution of the aluminum matrix. The four elements required for galvanic attack are certainly present. Specifically, these elements are the anode (the 6063 aluminum matrix), the cathode (the graphite fibers), the electrical connection

between them (they are in physical contact), and the electrolyte. So, the principal initiating corrosion mode on a completely unprotected composite is expected to be galvanic coupling.

Electrochemical test results confirm the conclusion that galvanic coupling between the graphite reinforcement and the aluminum matrix is the principal mode of corrosion in this composite when the edges are unprotected or when a pit propagates to an underlying fiber layer. A definitive way of evaluating the influence of the graphite fibers in the matrix is to overlay the Tafel slopes (obtained during the polarization studies) on a single plot and notice the shift in  $i_{\text{corr}}$  to increasing current densities when graphite fibers are present. This schematic is presented in Figure 22.

The first point borne out by the plot shown in Figure 22 concerns the relative magnitudes of the exchange current density of hydrogen reduction,  $i_0$ . As indicated in the results section,  $i_0$  for a composite surface foil or for the monolith in 3.5% sodium chloride was significantly increased when both aluminum matrix and graphite fibers were exposed to the electrolyte. This suggests that the substrate for the cathodic reaction changes from aluminum to graphite when graphite fibers are exposed in conjunction with aluminum, increasing  $i_0$  and  $i_{\text{corr}}$ . The exchange current density increase is attributed to the hydrogen reduction reaction occurring on the exposed graphite fibers (as they are more noble to aluminum) as opposed to occurring on the aluminum matrix. If the hydrogen reduction reaction were to continue on the aluminum matrix instead of the simultaneously exposed graphite fibers, then there would have been no coupling between the aluminum and the graphite and as a result no shift in  $i_0$  would have been observed.

Corrosion current densities associated with cross section exposed samples are considered galvanic corrosion current densities ( $i_{\text{galv}}$ 's) in this analysis. As seen in Figure 22, a shift to greater corrosion current densities was seen in both the sodium chloride and the sodium sulfate electrolytes. The same relative shift was observed when the composite

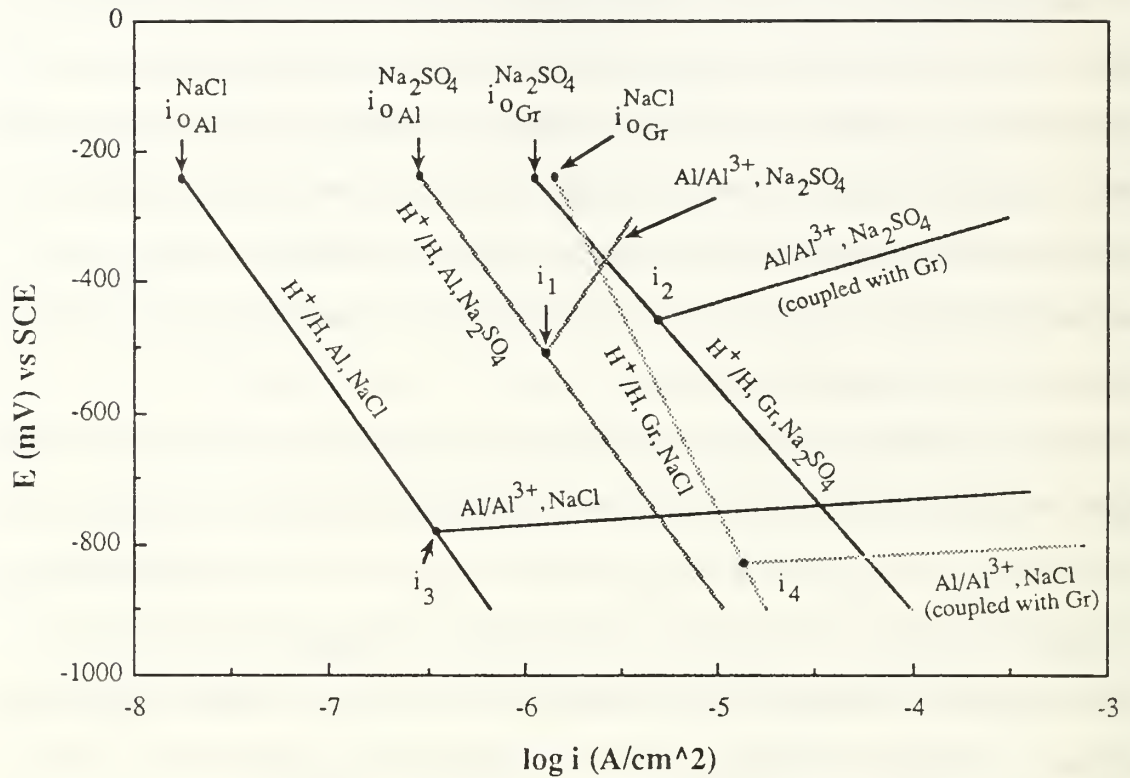


Figure 22: Corrosion model for the composite in 3.5% sodium chloride and 5.0% sodium sulfate developed from polarization tests performed on the 6063 aluminum monolith and the composite cross section

- Legend:
- $i_1$  is the corrosion current density for the monolith in 5.0% sodium sulfate
  - $i_2$  is the corrosion current density for the composite cross section in 5.0% sodium sulfate
  - $i_3$  is the corrosion current density for the monolith in 3.5% sodium chloride
  - $i_4$  is the corrosion current density for the composite cross section in 3.5% sodium chloride

$$i_2 \sim 5 * i_1 \text{ and } i_4 \sim 35 * i_3$$

surface foil data were overlayed on the cross section data. Slight differences in the Tafel slopes and  $i_0$  values add up to the significant shift in corrosion current densities. This consistent trend of increasing current densities from  $i_{\text{corr}}$  to  $i_{\text{galv}}$  lends additional support to the conclusion that galvanic coupling is important in this composite.

The polarization results indicating the regions of initial matrix dissolution as being localized do not run contrary to the theory of galvanic coupling. These results simply show that upon light anodic polarization specific high energy regions are subject to attack first. This can be explained on the basis of anodic and cathodic rates of reaction and how they are affected by anodic polarization. Upon anodic polarization, the anodic reaction rate is raised depending upon the magnitude of  $\beta_a$ . High energy interfaces and zones (such as surface precipitates and grain boundary particles) will be the first regions affected. At the same time, the cathodic reaction rate is reduced. As the degree of polarization is raised, the anodic and cathodic reaction rates become more separated (from their value at the free corrosion potential,  $E_{\text{corr}}$ ). This will result in a masking of the effect of galvanic coupling which is a process that will only occur to its fullest extent at the free corrosion potential.

In summary, a variety of tests were devised to show that galvanic coupling in this composite is important (in aqueous environments). Polarization studies and immersion tests were used. A careful and comprehensive analysis of the results of these tests including generous application of the principles of electrochemical theory has provided the means of elucidating the role of galvanic corrosion.

## **IV. EFFECT OF ENVIRONMENTAL AND MATERIAL VARIABLES**

### **A. RESULTS**

The complete set of behavior study data can be seen in parts (A), (B), and (C) of Table 2. Results given in parts (A) and (B) of the table were obtained with the 3.5% sodium chloride electrolyte deaerated. Part (C) of the table contains the results obtained by LT J. D. King in his master's thesis [Ref. 4]. The behavior data tabulated here is from testing conducted with an aerated 3.5% sodium chloride electrolyte. All solutions were buffered to either pH 4 or pH 8 as indicated in the second column of each part of the table. The matrix heat treatment of the composite tested is listed in the leftmost column.

### **B. DISCUSSION**

The effect of changing environmental and material variables (pH, presence or absence of sulfite ions, matrix heat treatment, and electrolyte aeration) on the corrosion behavior parameters ( $E_{\text{corr}}$ ,  $E_{\text{rep}}$ ,  $i_{\text{corr}}$ ,  $i_{\text{galv}}$ , and  $E_{\text{galv}}$ ) will be discussed here. And, since these behavior parameters are directly linked to pitting susceptibility, and general and galvanic corrosion rates, the discussion will primarily focus on how these three key measures of corrosion are affected by changes in one of the environmental or material variables. Because the analysis of the corrosion behavior of this composite is a complicated process, it will be split into an analysis of the composite's behavior in aerated and deaerated solutions, where the cathodic half-cell reactions, and hence the corrosion mechanisms, might be considerably different.

TABLE 2

## (A) ELECTROCHEMICAL TEST RESULTS IN 3.5% NaCl (DEAERATED)

Heat Treatment	Electrolyte pH	E <sub>corr</sub>	E <sub>rep</sub>	i <sub>corr</sub>	i <sub>galv</sub>	E <sub>galv</sub>
-T1	8	-950	-807	0.115	0.870	-860
-T6	8	-945	-811	0.529	0.844	-----
-W	8	-910	-804	0.972	0.568	-868
-T1	4	-811	-803	0.704	2.975	-806
-T6	4	-805	-799	1.56	-----	-788
-W	4	-810	-799	3.10	1.625	-785

(B) ELECTROCHEMICAL TEST RESULTS IN 3.5% NaCl (100 PPM SULFITE ION  
ADDED AND DEAERATED)

Heat Treatment	Electrolyte pH	E <sub>corr</sub>	E <sub>rep</sub>	i <sub>corr</sub>	i <sub>galv</sub>	E <sub>galv</sub>
-T1	8	-821	-808	0.236	0.217	-806
-W	8	-837	-810	1.24	0.230	-768
-T1	4	-797	-812	20.7	6.63	-804
-W	4	-804	-813	29.4	7.94	-766

## (C) ELECTROCHEMICAL TEST RESULTS IN 3.5% NaCl (AERATED)

Heat Treatment	Electrolyte pH	E <sub>corr</sub>	E <sub>rep</sub>	i <sub>corr</sub>	i <sub>galv</sub>	E <sub>galv</sub>
-T1	8	-775	-771	13.6	85	-770
-W	8	-795	-744	4.39	40	-750
-T1	4	-766	-764	41.1	350	-760
-W	4	-751	-768	15.1	250	-730

Units: E<sub>corr</sub>, E<sub>rep</sub>, and E<sub>galv</sub> measured in mV; i<sub>corr</sub> and i<sub>galv</sub> measured in  $\mu\text{A}/\text{cm}^2$

## 1. Corrosion Behavior in Deaerated Solutions

### *a. Effect of pH*

Results based on pH effect are valid for all three heat treatments and sulfite ion presence unless otherwise noted. The effects of heat treatment and sulfite ion addition will be treated separately in subsequent sections. As seen in Tables 2(A) and 2(B),  $E_{\text{CORR}}$  is more noble at pH 4 than at pH 8, and it is also evident that a change in pH between 8 and 4 has little or no effect on  $E_{\text{REP}}$ . The combination of these two results implies that the surface foils have good resistance to pitting at pH 8 because  $E_{\text{REP}}$  is considerably more electropositive than  $E_{\text{CORR}}$ . However, at pH 4 the surface foil is less resistant to pitting because  $E_{\text{CORR}}$  is almost equal to  $E_{\text{REP}}$  (in other words, a slight fluctuation in  $E_{\text{CORR}}$  may cause  $E_{\text{CORR}}$  to go greater than  $E_{\text{REP}}$  resulting in the inability of previously existing pits to repassivate). When sulfite ions are added,  $E_{\text{CORR}}$  becomes electropositive to  $E_{\text{REP}}$  at pH 4 making the surface foil considerably more susceptible to pitting. The probability of pitting is greater with sulfite ions present because none of the pits can repassivate. These results correlate with immersion test results.

When pH drops from 8 to 4, as seen in Tables 2(A) and 2(B),  $i_{\text{CORR}}$  increases probably due to passive film breakdown at pH 4. Referring to the Pourbaix diagram shown on page 3, the region of passivity of aluminum in pure water has its leftmost margin at pH 4. Therefore, in sodium chloride electrolytes, it is likely that this region of passivity will shrink, resulting in the oxide film becoming less stable at pH 4 than it would be if in pure water--thus causing the greater  $i_{\text{CORR}}$  values at pH 4 than at pH 8.  $E_{\text{GALV}}$  shows the same trend as  $E_{\text{CORR}}$  i.e., at pH 4  $E_{\text{GALV}}$  is more noble than at pH 8. At any given pH, heat treatment, or sulfite ion presence,  $E_{\text{GALV}}$  is electropositive relative to  $E_{\text{CORR}}$  since galvanic coupling polarizes the aluminum electropositively. Galvanic corrosion current density

( $i_{galv}$ ) increases at pH 4, following the same trend as  $i_{corr}$ . The rates of both galvanic and general corrosion are greater at pH 4 than at pH 8.

With sulfite ions present, a change in pH from 8 to 4 has no effect on  $E_{galv}$  (Table 2(B)). Although this is apparently contrary to what was found in the absence of sulfite ions (Table 2(A)), a close examination suggests that this is actually consistent with what is expected, as elucidated below. In the absence of sulfite ions with the matrix in the T1 condition, for example,  $E_{corr}$  shifted electropositively by 139 mV as the pH changed from 8 to 4. The corresponding electropositive shift in  $E_{galv}$  was substantially less at 54 mV. With sulfite ions present, on the other hand, the electropositive shift in  $E_{corr}$  for the T1 condition due to a change of pH from 8 to 4 was only 24 mV. So, the corresponding change in  $E_{galv}$  in the presence of sulfite ions would be expected to be negligible.

The susceptibility to localized corrosion and the rates of both general and galvanic corrosion were found to increase significantly when lowering pH from 8 to 4 for all heat treatments and with or without the presence of sulfite ions.

#### *b. Effect of Sulfite Ion Presence*

Corrosion potential ( $E_{corr}$ ) values are all shifted to more noble potentials when sulfite ions are present (Tables 2(A) and 2(B)). The shift at pH 4 is lower, however.  $E_{rep}$  is slightly more electronegative in the presence of sulfite ions, but with  $E_{rep}$ , the more significant change is at pH 4. The combined effects of  $E_{rep}$  and  $E_{corr}$  result in a lowering of the pitting resistance in the presence of sulfite ions. Also, the addition of sulfite ions results in an increase in  $i_{corr}$  at all heat treatments and pH levels (Tables 2(A) and 2(B)).

At pH 8, the addition of sulfite ions has a very small effect on  $i_{galv}$  (Sulfite ion addition seems to decrease  $i_{galv}$  slightly, although this effect is difficult to ascertain since the currents involved are very small. At pH 8, the principal cathodic reaction is expected to be oxygen reduction, the possibility of which is minimal due to deaeration,

resulting in the low observed  $i_{\text{corr}}$  and  $i_{\text{galv}}$ ). At pH 4, the addition of sulfite ions causes  $i_{\text{galv}}$  to increase significantly (Tables 2(A) and 2(B)). This is consistent with the increase seen in  $i_{\text{corr}}$  upon sulfite addition.  $E_{\text{galv}}$  shifts in the electropositive direction due to the addition of sulfite ions and this is consistent with the electropositive shift in  $E_{\text{corr}}$  in the presence of sulfite ions.

In summary, the presence of sulfite ions at pH 8 has little effect on the overall corrosion behavior of the composite, however, at pH 4 the presence of sulfite ions reduces pitting resistance and increases the rates of both general and galvanic corrosion. At pH 4 the protective oxide film on aluminum is less stable than at pH 8 as suggested by the Pourbaix diagram. The addition of sulfite ion has a further destabilizing effect on the film resulting in the observed deterioration in the pitting resistance. This is apparent from a comparison of Figures 5 and 8, as discussed in section III.A. The increase in  $i_{\text{galv}}$  and  $i_{\text{corr}}$  in the presence of sulfite ions can probably be attributed to the same effect.

### *c. Effect of Heat Treatment*

As shown in Tables 2(A) and 2(B), heat treatment seems to have little effect on  $E_{\text{corr}}$  and  $E_{\text{rep}}$  and therefore little effect on pitting susceptibility. It is observed from Table 2(A) that the maximum  $i_{\text{corr}}$  is obtained with the matrix in the -W condition, while intermediate  $i_{\text{corr}}$ 's and minimum  $i_{\text{corr}}$ 's are obtained with the matrix in the -T6 and -T1 conditions, respectively. This suggests that the general corrosion rate decreases with progressive aging. The same trend is observed in Table 2(B) for a 3.5% sodium chloride solution with 100 ppm sulfite ion addition.

In the absence of sulfite ions,  $i_{\text{galv}}$ , on the other hand, seems to increase slightly with aging, although to a much lesser extent than the decrease in  $i_{\text{corr}}$  (Table 2(A)). Little effect of heat treatment on  $i_{\text{galv}}$  is observed when sulfite ions are present in the electrolyte (Table 2(B)). This indicates that the effect of heat treatment in the rate of

galvanic corrosion is minimal. The galvanic corrosion potential ( $E_{galv}$ ) is relatively insensitive to heat treatment in the absence of sulfite ions (Table 2(A)), but becomes somewhat more noble in the presence of sulfite ions (Table 2(B)).

In summary, heat treatment has little effect on the susceptibility to localized corrosion at a given pH. The rate of general corrosion, however, was found to decrease appreciably due to progressive aging. The rate of galvanic corrosion between aluminum and graphite is affected little by heat treatment. If galvanic corrosion is a dominant mechanism of corrosion (i.e., when graphite and aluminum are simultaneously exposed to the electrolyte), then matrix heat treatment is not expected to have a significant impact on the corrosion behavior of the composite. If, on the other hand, the edges of the composite laminate are sealed (i.e., only the surface foil is exposed to the electrolyte), then the matrix should be heat treated to the -T6 condition or a slightly overaged condition to reduce the susceptibility to pitting and general corrosion.

## **2. Corrosion Behavior in Aerated Solutions**

There are some important differences in the composite's corrosion behavior when exposed to aerated solutions versus deaerated solutions (Table 2(C)). First, both  $E_{corr}$  and  $E_{rep}$ , are more noble in aerated solutions than in deaerated solutions. But the two are comparable at each pH level, making the composite susceptible to pitting at both pH 4 and at pH 8. Second, upon solutionizing and quenching (-W), the general and galvanic corrosion rates were found to decrease contrary to what was observed in deaerated solutions. The exact nature of such a behavior reversal is not understood at this point.

In addition, in aerated solutions, the magnitudes of both  $i_{corr}$  and  $i_{galv}$  are significantly greater than in deaerated solutions at both pH levels and all heat treatments. At pH 8 this is expected because oxygen reduction is the principle cathodic reaction at pH 8 and this reaction is minimal in deaerated solutions. In deaerated solutions at pH 4 the

hydrogen reduction reaction is the only feasible cathodic reaction. When the electrolyte (pH 4) is aerated, the oxygen reduction reaction ( $\text{O}_2 + 4\text{H}^+ + 4\text{e}^- \rightarrow 2\text{H}_2\text{O}$ ) becomes the primary cathodic reaction. Since both  $i_{\text{corr}}$  and  $i_{\text{galv}}$  are found to be greater in the pH 4 solution in the presence of oxygen, it can be inferred that the overall rate of the cathodic half-cell reaction is greater in the aerated solution, resulting in the observed acceleration in corrosion.

## V. CONCLUSIONS

The corrosion mechanisms and behavior of a P-130x graphite fiber reinforced 6063 aluminum composite laminate were studied. Depending upon the degree of exposure of the composite to its environment, one of two corrosion mechanisms will become important. In immersion tests, composite surface foils were found to be susceptible to pitting attack when just the composite edges were sealed. The surface foils showed good resistance to localized attack at pH 8, but at pH 4, with and without the presence of sulfite ions, the surface foils pitted after 10 weeks immersion in 3.5% sodium chloride. The presence of sulfite ions in solution results in a high pit density, but individual pit size remains small. Finally, pitting of the surface foils is important in harsh environments (e.g., chloride and sulfite ions present, in addition to low pH) and can eventually lead to galvanic corrosion.

If the composite edges were exposed to the electrolyte in addition to the surface foils, then galvanic coupling of the matrix and fibers became more important than pitting attack of the surface foils. This was true for both aqueous 3.5% sodium chloride and 5.0% sodium sulfate immersion studies after 10 weeks.

The behavior studies were all conducted in 3.5% sodium chloride solutions with varying pH (4 or 8), electrolyte aeration, matrix heat treatment, and presence of sulfite ion. The effects that changes in pH were seen to have on the corrosion behavior of the composite were significant. The susceptibility to localized corrosion and the rates of both general and galvanic corrosion increased significantly when lowering pH from 8 to 4. This effect was observed at all heat treatments and with or without the presence of sulfite ions.

The addition of sulfite ions, at pH 4, also reduced the composite's resistance to pitting and increased the rates of both general and galvanic corrosion. Heat treatment was found

to have little effect on the susceptibility to localized corrosion at a given pH, however, general corrosion rates were found to decrease appreciably due to progressive aging when the electrolyte is deaerated.

Electrolyte aeration results in a significant reduction in the composite's corrosion resistance to all forms of corrosion. For example, the composite was more susceptible to pitting at both pH 4 and pH 8, instead of just being susceptible to localized corrosion at pH 4 when the solution is deaerated. Both general and galvanic corrosion rates are substantially greater than in deaerated solutions at both pH levels and all heat treatments.

## REFERENCES

1. MMCIAC, *Introduction to Metal Matrix Material*, MMCIAC #272, p. 2-2, 1982.
2. Kreider, K. G., in *Introduction to Metal-Matrix Composites*, Kreider, K. G., ed., pp. 1-8, Academic Press, 1974.
3. King, F., *Aluminium and its Alloys*, p. 253, Ellis Horwood Limited, 1987.
4. King, J. D., *Characterization of the Corrosion of a P-130x Graphite Fiber Reinforced 6063 Aluminum Metal Matrix Composite*, Master's Thesis, Naval Postgraduate School, Monterey, California, December 1989.
5. Hollingsworth, E. H., and Hunsicker, H. Y., in *Corrosion and Corrosion Protection Handbook*, Schweitzer, P. A., ed., pp. 111-145, Marcel Dekker, Inc., 1983.
6. Kucera, V., and Mattsson, E., in *Corrosion Mechanisms*, Mansfeld, F., ed., pp. 211-284, Marcel Dekker, Inc., 1987.
7. Fontana, M. G., and Greene, N. D., *Corrosion Engineering*, p. 54, McGraw-Hill, 1978.
8. Materials Advisory Group U.S. Army Material Command and NACE, Paper No. 29, *Corrosion of Electronic Equipment Aboard Naval Ships*, Bjelland, L. K., and Schuler, M. D., pp. 387-388, December 1972.
9. Isaacs, H. S., "The Localized Breakdown and Repair of Passive Surfaces During Pitting," *Corrosion Science*, Vol. 29, No. 2/3, pp. 313-323, 1989.
10. Tan, T. C., and Chin, D-T., "Polarization of Aluminum During AC Corrosion in Sulfate Solutions," *Journal of the Electrochemical Society: Electrochemical Science and Technology*, Vol. 132, No. 4, pp. 766-772, April 1985.
11. Elboudjaini, M. and others, "An Electrochemical Investigation of the Behaviour of Aluminum Alloys in Different Electrolytes," *Corrosion Science*, Vol. 30, No.8/9, pp. 855-867, 1990.
12. Mansfeld, F., and others, "Pitting and Passivation of Al Alloys and Al-Based Metal Matrix Composites," *Journal of the Electrochemical Society: Electrochemical Science and Technology*, Vol. 137, No. 1, pp. 78-82, 1990.
13. Trzaskoma, P. P., "Aqueous Corrosion of Metal-Matrix Composites," *Journal of Metals*, Vol. 40, pp. 21-23, December 1988.

14. Himbeault, D. D., Varin, R. A., and Piekarski, K., "Coating of Graphite Fibers with Tungsten Carbide Using Solid and Liquid Copper as a Transfer Medium," *Metallurgical Transactions A*, Vol. 19A, pp. 2109-2113, August 1988.
15. Vassilaros, M. G., and others, in *Mechanical Behavior of Metal-Matrix Composites*, Hack, J. E., and Amateau, M. F., eds., pp. 335-353, TMS-AIME, 1983.
16. Pfeifer, W. H., in *Hybrid and Select Metal Matrix Composites: A State-of-the-Art Review*, Renton, W. J., ed., pp. 231-255, American Institute of Aeronautics and Astronautics, 1977.
17. American Society for Testing and Materials, ASTM Special Technical Publication 864, *Recent Advances in Composites in the United States and Japan*, Aylor, D. M., and Kain, R. M., pp. 632-647, June 1983.
18. Metzger, M., and Fishman, S. G., "Corrosion of Aluminum-Matrix Composites. Status Report," *Industrial Engineering Chemistry Product Resources Development*, Vol. 22, pp. 296-302, June 1983.
19. Trzaskoma, P. P., "Corrosion Behavior of a Graphite Fiber/Magnesium Metal Matrix Composite in Aqueous Chloride Solution," *Corrosion*, Vol. 42, pp. 609-613, October 1986.
20. Naval Sea Systems Command, Materials and Structures Division, Research and Technology Directorate, *The Corrosion of 6061 Aluminum Alloy--Thornel 50 Graphite Composite in Distilled Water and NaCl Solution*, by D. L. Dull, W. C. Harrigan, Jr., and M. F. Amateau, pp. 7-16, 6 May 1975.
21. Aylor, D. M., and Moran, P. J., "Effect of Reinforcement on the Pitting Behavior of Aluminum--Base Metal Matrix Composites," *Journal of the Electrochemical Society: Electrochemical Science and Technology*, Vol. 132, pp. 1277-1281, June 1985.
22. Aylor, D. M., and Moran, P. J., "Pitting Corrosion Behavior of 6061 Aluminum Foils in Sea Water," *Journal of the Electrochemical Society: Electrochemical Science and Technology*, Vol. 133, pp. 949-951, May 1986.
23. Office of Naval Research, *Localized Corrosion Induced in Graphite/Aluminum Metal--Matrix Composites by Residual Microstructural Chloride*, by L. H. Hihara and R. M. Latanision, pp. 1-13, February 1990.
24. Sedriks, A. J., Green, J. A. S., and Novak, D. L., "Corrosion Behavior of Aluminum--Boron Composites in Aqueous Chloride Solutions," *Metallurgical Transactions*, Vol. 2, pp. 871-875, March 1971.
25. Trzaskoma, P. P., and McCafferty, E., "Corrosion Behavior of SiC/Al Metal Matrix Composites," *Journal of the Electrochemical Society: Electrochemical Science and Technology*, Vol. 130, pp. 1804-1809, September 1983.

26. Trzaskoma, P. P., "Pit Morphology of Aluminum Alloy and Silicon Carbide/Aluminum Alloy Metal Matrix Composites," *Corrosion*, Vol. 46, pp. 402-409, May 1990.
27. National Association of Corrosion Engineers, NACE Standard TM-01-69, *Laboratory Corrosion Testing of Metals for the Process Industries*, 1969.
28. EG&G Princeton Applied Research, *Model 351 Corrosion Measurement System Preliminary Operating Manual*, 1985.
29. Hirozawa, S. T., "Galvanostaircase Polarization", *Journal of the Electrochemical Society: Electrochemical Science and Technology*, Vol. 130, pp. 1718-1721, August 1983.
30. American Society for Testing and Materials, "Standard Test Method for Conducting Cyclic Galvanostaircase Polarization," Designation: G 100-89, *Annual Book of ASTM Standards*, pp. 260-262, 1989.

## INITIAL DISTRIBUTION LIST

	No. Copies
1. Defense Technical Information Center Cameron Station Alexandria, VA 22304-6145	2
2. Library, Code 52 Naval Postgraduate School Monterey, CA 93943-5002	2
3. Department Chairman, Code ME Department of Mechanical Engineering Naval Postgraduate School Monterey, CA 93943-5000	1
4. Naval Engineering Curricular Office, Code 34 Naval Postgraduate School Monterey, CA 93943-5000	1
5. Professor I. Dutta, Code ME/Du Department of Mechanical Engineering Naval Postgraduate School Monterey, CA 93943-5000	3
6. LT Leslie R. Elkin, USN 1804 Twin Oaks Lane Lafayette, IN 47905	1
7. Mr. Kevin G. Beasley Electronic Development Department Naval Weapons Support Center Crane, IN 47522	1
8. Dr. Patricia P. Trzaskoma Surface Protection Section Code 6322 Material Science and Technology Division Naval Research Laboratory Washington, DC 20375	1





3 2768 00005178 3